Predictability as Principle of Control in Interaction with Complex Objects

by

Tri Nguyen

A Dissertation Presented in Partial Fulfillment
of the Requirements for the Degree
Doctor of Philosophy

Approved November 2022 by the
Graduate Supervisory Committee:

Arthur Glenberg, Co-Chair
Eric Amazeen, Co-Chair
Polemnia Amazeen
Gene Brewer

ARIZONA STATE UNIVERSITY

December 2022

ABSTRACT

Recent findings in human interactions with complex objects, objects with unpredictable interaction dynamics, revealed predictability as an important factor when determining effective control strategies. The current study extended these findings by examining the role of predictability in the selection of control strategies in two scenarios: during initial interactions with a novel, complex object, and when intentional constraints are imposed. In Experiment 1, methods with which people can identify and improve their control strategy during initial interactions with a complex object were examined. Participants actively restricted their movements at first to simplify the object's complex behavior, then gradually adjusted movements to improve the system's predictability. In Experiment 2, predictability of participants' control strategies was monitored when the intention to act was changed to prioritize speed over stability. Even when incentivized to seek alternative strategies, people still prioritized predictability, and would compensate for the loss of predictability. These experiments furthered understanding of the motor control processes as a whole and may reveal important implications when generalized to other domains that also interact with complex systems.

TABLE OF CONTENTS

Page

LIST OF FIGURES iv

CHAPTER

1 INTRODUCTION 1

The Degree of Freedom Problem in Motor Control 1

Degrees of Freedom in Control and Manipulation of Tools 5

Predictability as Principle of Control in the Cart-Pendulum Model 7

Implementation of the Cart-Pendulum Model 10

2 EXPERIMENT 1 13

Methods..15

Results..21

Discussion..39

3 EXPERIMENT 2 42

Methods..45

Results..49

Discussion..58

4 CONCLUSION 61

Limitations and Future Directions 63

Conclusion 65

REFERENCES 66

Page

APPENDIX

A. IMPROVEMENTS TO CART-PENDULUM MODEL TO ACCOMMODATE HYBRID MOVEMENT PATTERN 73

LIST OF FIGURES

Figure Page

1. Predictability Landscape at Different Pendulum Weights 18

2. Raw Data and Preliminary Analyses for Participant 5, Trial 2. 23

3. Model Predicted Signals Versus Observed Signals for Participant 5, Trial 2 24

4. Raw Data and Preliminary Analyses for Participant 14, Trial 34. 25

5. Model Predicted Signals Versus Observed Signals for Participant 14, Trial 34.... 26

6. Raw Data and Preliminary Analyses for Participant 3, Trial 10 27

7. Model Predicted Signals Versus Observed Signals for Participant 3, Trial 10...... 28

8. Parameter State Space Showing Mutual Information at Different Values of K, B, and m_p 30s

9. Line Graph Showing Movement Amplitudes over Trials 32

10. Parameter State Space Showing Mutual Information at Different Values of K, B, and Amplitude A 32

11. Quiver Plot Showing Each Participant's Average Strategy.................................... 34

12. Raincloud Plot Showing Absolute Mutual Information 35

13. Raincloud Plot Showing Relative Mutual Information 36

14. Line Plot Showing Distance to Local and Global Maxima per Quantile 37

15. Line Graph Showing Mean Distance to Local (Adjusted with Movement Amplitude) Maxima Versus Distance to Global Maximum over Quintiles and Model Complexity 39

16. Parameter State Space Showing the Lissajous Linear Regression Slope for Each K/B Parameter Pair 48

Figure Page

17. Parameter State Space Showing Mutual Information at Different Values of K and B..52

18. Line Graph Showing Observed Frequency in Each Trial.......................................54

19. Line Graph Showing Average Distance to the Global Maximum and the Antiphase Maximum for Selected Strategies per Quintiles....................................55

20. Comparisons of Absolute Mutual Information Between Experiment 1 and 2.......56

CHAPTER 1

INTRODUCTION

Effective control of the human body's multitude of degrees of freedom is a long-standing question in motor control. Several competing theories attempted to explain how we can control our body's movements with flexibility and stability. Recent studies highlighted the utility of studying interactions with external complex systems, many of which exhibit nonlinear, chaotic behaviors, to reveal generalized principles of motor control. What principles of control are utilized in interactions with complex systems? How do people apply these principles to control unpredictable objects? In this set of experiments, we examined the principle of predictable control in movement interactions with the fluid-in-a-cup system in two scenarios: when information about the system is limited, and when additional constraint is imposed.

The degree of freedom problem in motor control

Bernstein (1967) highlighted the large number of degrees of freedom involved in movements as a key issue that must be addressed in theories of motor control. Specifically, movements depend on muscles (which differ in length, strength, orientation, type, level of fatigue, etc.), architecture (tendon length and elasticity), skeletal structure (joint angle, mechanical advantage of tendon-joint pairs) (Scott, 2004). This is further complicated by multiple control pathways to both local (spinal) and central (cortical) nervous systems. Finally, the amount of force each muscle group needs to apply also must take into account the current angle and velocity of the limb, the effect of gravity on the current limb orientation, as well as any additional constraints imparted by external forces or objects of interaction. In effect, an important part of the question of motor control can be reframed as: how can a system's degrees of freedom be reduced, and therefore converted into a controllable or predictable state?

Two main approaches have emerged as potential solutions to this question: centralized control and dynamical systems theory (Schaal, Mohajerian, & Ijspeert, 2007). One solution for the degree of freedom problem from the centralized control approach involves generalized motor programs (Schmitt, 1975, 1985), which account for the generativity of movement (the ability to replicate a movement under novel circumstances) by grouping movements into classes according to the relative timing of each movement segments. Abstraction and categorization of equivalent action classes effectively reduce the system's degrees of freedom, while variable parameters allow for generalization of action classes to different execution scenarios. Action classes acquisition, selection, and parameter tuning are defined at the executive (top-down) level (Turvey, 1990). However, critics have pointed out several areas where a centralized control approach may not be adequate in accounting for human movement behaviors. For example, while generalized motor programs alleviated the storage problem with its focus on relative characteristics of movement, itself an improvement on Adam's (1971) closed-loop motor control theory, it did not go far enough (Kugler & Turvey, 1978; Newell, 2003; Shae & Wulf, 2005). Questions over the format as well as the need to rely on internal abstract models and programs were also regularly raised.

In an effort to move away from the centralized control approach, several alternative theories were proposed from a perspective where other aspects of the motor system potentially play a role in reducing the number of degrees of freedom. For example, Bernstein (1967) postulated that the motor system freezes degrees of freedom at the biomechanical periphery upon encountering a novel situation (see Newell & Vaillancourt (2001) for a review of empirical evidence). Several researchers also emphasized consideration of the inherent dynamics of the peripheral systems and constraints imposed by external factors in solving the degree of freedom problem (Heuer, 1994; Mitra, Amazeen, & Turvey, 1998; Newell & Vaillancourt, 2001). Evidence substantiating these theoretical considerations can be found in studies on joint coordination in writing and drawing (Lacquaniti, 1989), coordination dynamics in bimanual pendulum swing (Mitra et. al., 1998), uncontrolled manifold in postural control (Scholz & Schoner, 1999), muscle synergy in animal movement (d'Avella, Saltiel, & Bizzi, 2003; Ting & McKay, 2007), among others. Research from the dynamical systems approach shares a common thread: decentralizing reliance on internalized models and shifting explanatory power to the materials, structure, and coupling between the body and the environment.

Both centralized control and dynamical systems approaches led to a wealth of models that aim to capture motor behaviors. The general centralized control framework is consistent with the optimal control modelling approach. This approach assumes that people acquire and operate upon accurate internal models of the system. Parameters needed to execute an action can then be obtained by optimizing the model based on a general organizational principle such as minimizing expended energy or minimizing error (Schaal, Mohajerian, & Ijspeert, 2007). Similar to the theoretical discussion, efforts to implement centralized control perspective in modelling also ran into issues. One, given the large number of degrees of freedom, solutions for vectors of control parameters are either computationally expensive or intractable. Two, centralized models perform well in static or fully predictable environments but poorly in situations where the environmental dynamic changes, or when deviations to the generated plan occurs and reactive control is needed (Desmurget & Grafton, 2000; Schaal et. al., 2007).

Models within the dynamical systems perspective typically focused on relational (coupling) terms, which is inherently an exercise in reduction of degrees of freedom (Haken, Bunz, & Kelso, 1985; Kugler & Turvey, 1987; Rand, Cohen, & Holmes, 1988; Amazeen, Amazeen, & Turvey, 1998). This approach also allows for quantification of the evolution (dynamics) of the motor system over the time course of a movement, while taking into account both perceptual information (and thus feedback), innate biomechanical properties of the system, and external constraints. For example, Thelen and Smith (1993) incorporated memory processes (delay between stimulus presentation and action), motor control maturity (developmental age), and salience of visual stimuli (distance or color) into a unified dynamic field model that was able to accurately account for a wide range of behavioral data for toddler's A-not-B errors (see also Thelen, Schoner, Scheier, & Smith, 2001). Both discrete movements (such as pointing or reaching) and more cyclic movements (such as walking) can be modeled as vectors of system state dynamics (that gravitate towards a single state or towards a series of bounded, recurring states, respectively, see discussion of attractors in Abraham & Shaw, 1992).

Regardless of perspective, it is clear that the degree of freedom problem is an important, and still ongoing issue in motor control. This question is further complicated when we consider interactions with tools. Even simple tools come with unique physical characteristics and additional degrees of freedom. Yet most people are able to quickly intuit the natural dynamics of novel tools or objects and learn to control and manipulate them without much difficulty. For instance, Mitra, Amazeen, and Turvey (1998) cited the example of learning to ride a bike. With five controllable parts, riding a bike requires users to understand the dynamics and simultaneously control ten degrees of freedom (one DOF to describe the part's current state, and one more to describe its trajectory). The authors posed an interesting question: Is the intuition that a rider gain the same as the acquisition of a single (or a few) variable that fully accommodate all ten degrees of freedom? In light of the discussion thus far, this question can be reframed as: Is learning to control a tool utilizing the same principle of reducing degrees of freedom as learning to control the body? If so, experiments on tool use present a window of opportunity that can be utilized to examine principles of motor control in general.

Degrees of freedom in control and manipulation of tools

Given that most tools have finite and easily identifiable degrees of freedom, most theories on tool use have favored a centralized control approach, with some extensions to consider peripheral and external effects. For example, the reasoning-based approach (Osiurak & Badets, 2016; Goldenberg, 2013) argued that properties of a tool are analyzed and obtained from sensory information, then stored in semantic memory. When an interaction with the tool is considered, knowledge of the tool is combined with abstract mechanical knowledge of the task and general knowledge of physics to form a mental simulation of possible outcomes. The result of this mental simulation then informs motor simulation, which then becomes action execution. Alternatively, the manipulation-based approach (Buxbaum, 2001; Thill, Caligiore, Borghi, Ziemke, & Baldassarre, 2013) attempted to account for the degrees of freedom problem by suggesting that stored knowledge of a tool's canonical use is retrieved to bias perceptual information about a tool being considered for action (for empirical examples, see Tucker & Ellis, 1998 and Symes, Ellis, & Tucker, 2007). This allows for past experiences to constrain possible control strategies for tool manipulation. Both the reasoning-based and the manipulation-based approaches rely on centralized internal models and encoded knowledge for simulation and execution of interactions with tools.

A third view, the embodied approach, took the dynamical systems perspective and moved away from centralized control explanation by arguing that a tool's physical and functional properties alter the parameters of our peripheral models (Martel, Cardinali, Roy, & Farnè, 2016; Osiurak & Badet, 2016). For example, Cardinali et. al. (2009) demonstrated in a series of experiments that after using a grabbing tool for a short period of time, participants perceived their arms to be longer than usual and exhibited kinematics similar to people with long arms (see also Pagano, 1993; Baccarini, Martel, Cardinali, Sillan, Farnè, & Roy, 2014). By encoding (in the body schema construct) the effects of tool use on the dynamics of movement at the periphery, this approach avoided requiring people to obtain and maintain an accurate internal model of the tool system. Furthermore, monitoring the combined effects of all degrees of freedom in a tool system on the effector may prove to be critical in solving the degree of freedom problem in interactions with tools and other external objects.

Most studies on tool use have focused on simple, rigid objects (Flanagan & Wing, 1997; Maravita, & Iriki, 2004; Cardinali et. al., 2009; Slota, Latash, & Zatsiorsky, 2011) In the relatively few studies on complex objects (balancing stick/inverted pendulum in Cabrera & Milton, 2004; compressing buckling spring in Mosier, Lau, Wang, Venkadesan, & Valero-Cuevas, 2011), the movements studied were often short and discrete, which limited our ability to examine the evolution of system dynamics over time. Complex, nonlinear systems operating in dynamic environment exhibit sensitivity to conditions and perturbations, which require flexibility in control strategies to produce online reactions (Schaal et al., 2007). Traditional models of tool use struggled to capture the dynamics of such systems.

Overall, a parallel can be drawn between the literature on motor control and tool use. Both utilized models from either the centralized control approach or the dynamical systems approach to tackle the question of control. Studies on tool use have mostly focused on simple tools, thus avoiding the degree of freedom issue. However, recent studies provided some answers on how this issue can be solved in interactions with nonlinear, unpredictable tool systems, which more closely resemble the complexity of the body.

Predictability as principle of control in the cart-pendulum model

A recent line of research focused on the principle of control of a complex, unpredictable tool system: a continuously moving cart-pendulum system (Wallace, Kong, Rodriguez, & Lai, 2021; Maurice, Hogan, & Sternad, 2018; Bazzi & Sternad, 2020). The system is modeled after the task of transporting a cup of water from point A to point B, something we do every day. As the cup moves, force is transferred to the liquid within, which reacts in an unpredictable manner and imparts force back against the cup. This, in turn, has an effect on the amount of force transferred to the liquid in the next instant. Thus, this system represents a class of objects that has nonlinear and chaotic interaction dynamics. An understanding of interactions with this class of object can provide important insight on how people approach control of complex systems in general.

Despite the complexity and diverse patterns of behavior of the fluid-in-a-cup system, most people have no problem interacting with this system daily. However, accurate modeling and simulation of this complex system have proven to be a slow and taxing task computationally. How, then, can we explain our ability to quickly grasp how to control this system, maintain stability for long periods of time, and fluidly react to sudden perturbation? Maurice et. al. (2018) provided an answer by showing that people opted for strategies with the highest amount of predictability instead of strategies that minimize traditional optimization goals such as force expenditure or jerkiness (Dingwell et. al., 2004; Svinin, Goncharenko, Kryssanov, & Magid, 2019; see also, Bazzi & Sternad, 2020). Even when the system's complexity allowed for two distinct patterns of movement with high predictability (in phase with the pendulum, or anti-phase with the pendulum), people opted for one of the two strategies, while avoiding options in between. Bazzi and Sternad (2020) further found that participants gravitated towards highly predictable strategies over the course of the experiment, suggesting that participants were able to evaluate the predictability of a given movement strategy.

Predictability is an oft discussed concept in dynamics systems theory and shares a close root to Bernstein's notion of the degree of freedom problem. For example, Abraham and Shaw (1992) highlighted the utility of attractor reconstruction techniques in observing and characterizing patterns of behaviors in a system, thus enabling prediction of system dynamics over potentially extended time intervals. A system in a stable attractor rejects momentary noise or perturbations and does not overly rely on constant, precise, and computationally heavy closed-loop control (Bazzi & Sternad, 2020). Experimentally, stability (one of many ways predictability is defined) is prominently featured in studies of motor control in posture and balance (Roerdink, De Haart, Daffertshofer, Donker, Geurts, & Beek, 2006; Stergiou & Decker, 2011; Gibbons, Amazeen, & Jondac, 2019).

Control through predictability addresses the degree of freedom issue in interactions with complex objects in two ways. One, predictability quantifies the relationship between the input control vector and the output tool behavior, thus allowing us to use only one variable to describe the system's behavior instead of two (one for the input, and one for the output). This parsimony is the inherent advantage in using relational terms to capture a system's dynamics. Two, predictability simultaneously captures the dynamics of both complex systems under consideration: the body and the complex object. The input control vector is the product of the nested interactions of the body's degrees of freedom, whereas the output tool vector is the product of interactions between the cart-pendulum system's degrees of freedom. Predictability thus represents the dynamics of the whole agent-tool system with one parameter. Both the focus on relational terms and the combination of nested interactions into one order parameter are emblematic of the dynamical systems' approach to solving the degree of freedom issue (Mitra et al., 1998; Amazeen, 2018; see also, Thelen & Smith, 1993).

In this series of experiments, we examined whether the finding of predictability as a principle of control can be extended to two scenarios: when information about the system's dynamics is limited (such as during initial interactions), and when additional constraint is imposed on the system. In Experiment 1, we examined participants' control strategies during early interactions with a complex, nonlinear object and assessed how participants adjusted control strategies to achieve higher predictability. In Experiment 2, we manipulated the psychological aspect of the task to examine whether a shift in intention can influence participants' selection of control strategies. In both experiments, we utilized the cart-pendulum model to accurately quantify the control strategy selected during each trial and compare it with other possibilities.

Implementation of the cart-pendulum model

The cart-pendulum model is a mechanical model of the fluid-in-a-cup system that simplifies the challenging task of modeling the state of a 3-dimensional liquid, while maintaining the two key characteristics of the original system: underactuation (the number of actuators or inputs is fewer than the number of degrees of freedom) and nonlinearity (recursive interactions can sometimes result in chaotic behavior) (Bazzi & Sternad, 2020). The cart-pendulum model consists of a single cart moving on a bounded 2-dimensional track and a pendulum weight attached to the underside of the cart. When the cart is moved, force is transferred to the pendulum, which then swings in accordance with its own natural dynamics. The swinging motion imparts force back onto the cart, which changes the total amount of force transferred to the pendulum in the next instance of time. This process is allowed to recur over several cycles, providing us with a picture of the dynamic interactions between the input cart movement and the output pendulum movement.

The cart-pendulum system has two degrees of freedom: the displacement of the cart and the angular displacement of the pendulum (Wallace et. al., 2021). Thus, we need four variables to describe these degrees of freedom: the current state (position) of the cart and its rate of change (velocity), and the current state (position) of the pendulum and its rate of change (velocity). Furthermore, the cart-pendulum is being continuously driven by periodic force from the participants. Overall, the whole system requires five variables to completely describe.

The motion equations for the cart-pendulum system are given as a system of differential equations:

$$\ddot{x} = (m_p d\dot{\theta}^2 \sin(\theta) + m_p g sin(\theta)\cos(\theta) + F)/(m_c + m_p sin^2(\theta)) \qquad (1)$$

$$\ddot{\theta} = -\frac{\ddot{x}}{d}\cos(\theta) - \frac{g}{d} \qquad (2)$$

where x denotes the position of the cart, θ denotes the angular position of the pendulum, m_p is the mass of the pendulum, m_c is the mass of the cart, d is the length of the pendulum swing, and g denotes the gravitational acceleration.

The F term denotes the input force provided by the human subject. Given the task constraints, the driving force closely follows a sinusoidal goal trajectory of the cart:

$$x_{des}(t) = Asin(2\pi f t + \frac{\pi}{2}) \qquad (3)$$

which results in an input force

$$F_{input}(t) = (m_c + m_p)\ddot{x}_{des}(t) \qquad (4)$$

Maurice, Hogan, and Sternad (2018) noted that this cart-pendulum model did not take into account the neuro-mechanical properties of the human subject. Therefore, an additional term was added to model the impedance of the hand interacting with the cart using a mass-spring model, where K represents spring stiffness and B represents damping or friction.

$$F = F_{input} - K(x - x_{des}) - B(\dot{x} - \dot{x}_{des}) \qquad (5)$$

Since the interactions between the cart and the pendulum can be fully captured by physics, the human participant's control strategy while interacting with this system can be described by a vector of 4 parameters: *A* (amplitude of the cart movement), *f* (frequency of cart oscillation), *K* (hand stiffness), and *B* (hand damping). Of these four parameters, *A* and *f* can be observed and measured directly from movement data, while *K* and *B* are latent and have to be estimated. This model then allows us to efficiently describe participants' chosen strategies. It also allows us to compare these strategies against alternative, unobserved strategies and evaluate their relative performance on a variety of objective functions. Since our objective is to investigate the role of centralized control processes while predictability is guiding interactions with the systems, we used predictability as our main objective function.

Predictability can be quantified as the amount of mutual information between two variables. Mutual information, a concept from Shannon's (1948) information theory, refers to the statistical dependency between two variables, or how much observing one variable allows one to predict the other variable. If two variables have high mutual information, knowing one variable means there is less uncertainty about the other variable (Cover & Gopinath, 2012). Mutual information was used to quantify predictability in chaotic weather systems (Del Sole, 2004).

For our purpose, in Experiment 1, we looked at several simplified versions of the cart-pendulum model to see if participants' choices matched the simplified models' solutions. In Experiment 2, we measured the difference in selected control strategies when the participants' intention shifted to see how the predictability in selected strategies changed under additional system constraint.

CHAPTER 2

EXPERIMENT 1

Bazzi and Sternard (2020) showed that the predictability of participants' selected strategies during interactions with a complex object increased over time. That is, participants were able to adjust their control strategies and perform solutions with higher predictability. How was this process accomplished?

Naturally, the major issue with early interactions with any object is the fact that participants do not have full information about the system's physical properties as well as its reaction to control input. This problem is especially true for complex objects, which have complicated interaction dynamics and are sensitive to small changes in the control vector. There are two potential solutions to this problem. One, participants can use initial interactions with the system to estimate its physical properties. This information can then be used to construct a more accurate model of the system, which can be used to generate control strategies with higher predictability (through motor simulation). Two, participants can restrict initial interactions with the system to observe its dynamics, then gradually adjust their control strategy until the predictability between their input and the system's output improves. Participants may also utilize both methods to improve their control.

The first method is consistent with both the reasoning-based theory (Osiurak et al., 2010; Goldenberg, 2013; Osiurak & Badets, 2016) as well as with manipulation-based theory of tool use (Bauxbaum, 2001). Authors from these perspectives suggested that during interactions with novel tools, or with normal tools among patients with specific types of apraxia, new models of the tool systems are constructed from function knowledge, mechanical knowledge, as well as motor simulation (reasoning-based) or representations (manipulation-based). These models are then used to generate, plan, and execute motor behaviors.

The second method is consistent with the dynamical systems approach. Authors from this perspective suggested that a component of the process of attunement to and exploitation of a system's dynamic in motor control involves a reduction in the system's degree of freedom during the early stages of interaction (Bernstein, 1967; see Newell & Vaillancourt, 2001 for comprehensive review). For example, several studies reported arrest of joint segments during the initial learning stage of a movement task such as skiing (Vereijken, et. al., 1992), dart throwing (McDonald, Emmerik, & Newell, 1989) or prehension task (Steenbergen, Martennuik, & Kalbfleisch, 1995), followed by later relaxation of these restrictions in pistol shooting (Arutyunyan, Gurfinkel, & Mirskii, 1968), racquetball forehand shooting (Southard & Higgins, 1987), and arm movement task (Schneider & Zernicke, 1989). Several researchers have also suggested that reduction of system complexity should be viewed at a higher (dynamical) level, instead of at the joint-muscle level (Mitra et. al., 1998; Newell & Vaillancourt, 2001).

Authors from both perspectives clearly agreed that some forms of model simplification take place during early interactions with a novel system. For the centralized control approach, simple internal models of the systems are generated using logical rules and stored knowledge. For the dynamical systems approach, model simplification is achieved near the biomechanical periphery (joint-muscle level). In this experiment, we generated a series of simplified models of the cart-pendulum system using both approaches and examined whether participants' chosen control strategies were informed by such models. That is, if participants employed the model building method, we would expect to see their selected strategies clustered around regions of high predictability according to simplified models generated by using progressively more accurate physical measurements. If participants used the movement restriction method, we would expect to see their selected strategies clustered around high predictability regions according to simplified models with progressively less restrictive movements.

Methods

Participants

Human subjects (N = 14) were recruited from the Introductory Psychology student pool at Arizona State University to participate in the experiment. One subject dropped out during the experiment and was excluded from the analysis, resulting in a total sample size of 13.

Apparatus

The experimental design closely followed the design of Bazzi and Sternad's (2021) study 3 (section 6.1), with a few adjustments. A cart (m_c = 20 g) was placed on a suspended single-rail track. The track restricted the cart's movements to approximately 20cm in both lateral directions (with clearance on both sides). Suspended from the cart was a pendulum (m_p = 46 g) connected via wire of length 0.19 m. Movements of the cart and pendulum were tracked via two infrared-emitting diodes, with an Optotrak 3020 motion-capture camera recording movements at a sampling rate of 100Hz.

Procedure

Participants provided informed consent upon arrival at the lab. They were instructed to place their finger on top of the cart to oscillate the cart on the track so that the pendulum moved between two large target boxes. The target boxes were spaced so that the amplitude of the pendulum was free to range between 4cm and 20cm. A metronome paced the subject's movement so that each left-right, or right-left movement coincided with one beat. The frequency of the metronome beat was tuned to the resonant frequency of the cart-pendulum system (approximately 1Hz for this system). Participants were instructed that they could go faster than the metronome (to facilitate anti-phase strategies), but no slower (to avoid stationary strategies). Each subject performed 50 trials of 45 seconds each in one session. Participants performed in 5 blocks of 10 trials, with 15 seconds of rest between trials, and several minutes of rest between blocks. Power analysis using GPower suggested N = 10 to achieve power of .8 (repeated measures, within subject effect for two groups with 50 measurements, moderate effect size f = .15, α = .05). Upon completion of the trials, participants provided demographic information, then were debriefed and dismissed. The experimental procedure was approved by the Institutional Review Board at Arizona State University.

Modeling

Parameters of the cart-pendulum model can be separated into two categories: those controlled by the participants and those that were not. Parameters controlled by the participants all stemmed from the driving force term F (Eq. 5), which included K, B, A, and f. If participants restricted their movements to better grasp the system's dynamics, they would modify one of these parameters. K and B were latent parameters driven by A and f through the x_{des} term (Equation 3 and 5). The f parameter was restricted during the experiment. As such, A is the parameter that participants had the most control over and was used to generate simplified models of the movement restriction method.

Parameters that participants did not directly control specified the remaining four degrees of freedom of the cart-pendulum system: the cart's position and velocity, and the pendulum's position and velocity. The cart was a solid object that only moved in one dimension. As such, most participants should have ample experience to accurately model its behavior. The novel and unpredictable component of this system was the pendulum and its reaction to input forces generated by the participant. The reaction force between the cart and the pendulum is described by the equation (Bazzi & Sternad, 2021):

$$F_{pendulum} = m_p l(\dot{\theta}^2 \sin(\theta) - \ddot{\theta}\cos(\theta)) \qquad (6)$$

Within equation 6, only the m_p and l parameters can be modified (the rest are relational terms). Whereas l (the length of the pendulum link) can be directly observed, m_p (the weight of the pendulum) cannot be estimated without direct interaction. To a participant observing the physical model and attempting to construct a model of the system, m_p represented the most impactful missing parameter and the most logical target to be used for model simplification. Therefore, we modified m_p to generate simplified models for the model building method.

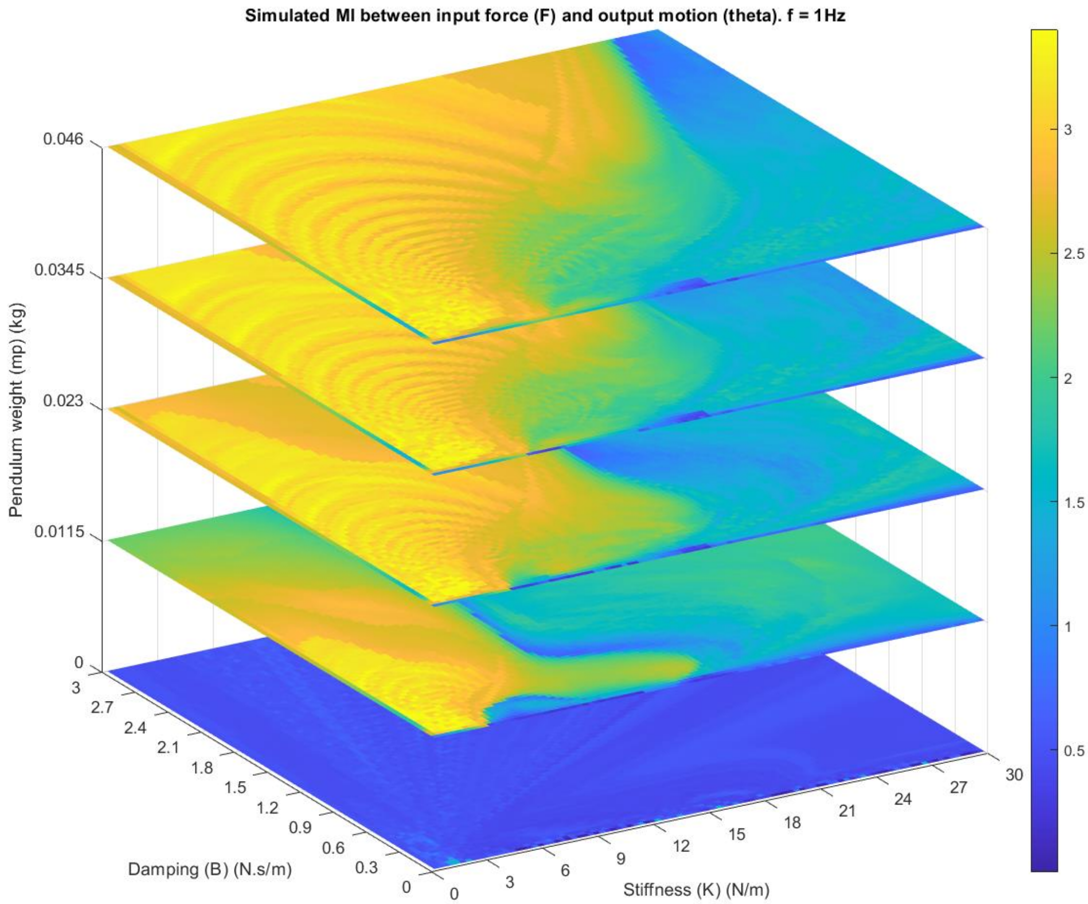

Figure 1. Predictability landscape at different pendulum weights (A = .03). The bottom layer represents predictability between input and out up if pendulum weight *mp* = 0. The top layer shows regions of high and low predictability that emerge as the dynamics of the system becomes stratified due to greater pendulum weight *mp* = .046.

The experimental setup fixed frequency f to a constant, and initial pendulum phase and phase velocity were both set to 0 at the start of each trial. Thus, each subject's selected strategy could be described using three variables: amplitude A, stiffness K, and damping force B. From participants' observed movement data, amplitude A was calculated based on recorded cart movement. K and B parameters were estimated by minimizing the root mean squared differences between model generated and observed data for four vectors: cart position, cart velocity, pendulum position, and pendulum velocity. The range for the A (from 0.01 to 0.03 meters), K (from 0 to 30 N/m), and B (from 0 to 3 N.s/m) parameters were obtained from empirical data. Finally, predictability was calculated between the input position vector and the output pendulum phase angle θ generated by the model.

To simulate all other unobserved movement strategies, simulated values for each of A, m_p, K, and B parameters (within the described range) were fed into the model to generate simulated cart vector and pendulum vector (according to equation 1 and 2). Simulated values were generated by sampling the K and B parameter ranges at 100 regular intervals, A at 3 levels (0.01, 0.02, and 0.03 meters), and m_p at 5 levels (0, 0.012, 0.023, 0.035, and 0.046kg). The calculated mutual information values were used to construct a state space where subjects' chosen execution strategies were mapped (see Figure 1 for example). The center point of the region with highest mutual information was calculated as the averaged coordinates of all points with mutual information exceeding the 75th percentile. This point was calculated for the full model (global maximum), which used parameters that matched the physical apparatus, as well as for each of the simplified models (local maxima), which used reduced pendulum weight parameters m_p or reduced amplitude A.

To test whether state spaces of simplified models matched observed strategies over time, for the model building method, clusters of observed strategies in the first ten trials were mapped onto the state space portrait with simplest dynamics (m_p = 0kg), followed by the next set of ten trials mapped on to the next level of system complexity (m_p = 0.012kg). This process was repeated until the model reached full complexity (m_p = 0.046kg) at the fifth quintile. For the movement restriction method, the first, third, and fifth quintiles were mapped onto the simplified models generated by using *A* at 0.01, 0.02, and 0.03, respectively.

Data processing and analysis

From the raw 3-D signals of cart and pendulum movements, the lateral and vertical vectors of each component were isolated and subjected to a 5-point smoothing function to remove minor instrument errors. The first 5 seconds of each 45-second trial was also trimmed to remove startup transients. After centering and standardizing, we calculated the velocity vectors from the position vectors of the cart and the pendulum. The lateral and vertical vectors for the pendulum were used to calculate the phase angle and phase angle velocity of the pendulum's movements. A standard sine wave function was used to estimate the amplitude and frequency of oscillations in the cart position signal. An example fit between observed cart position and estimated sine wave fit is shown in Figure 2, panel B. Additionally, a Lissajous plot (mapping cart position against pendulum position), phase portrait (mapping cart velocity against pendulum position), and relative phase histogram (showing frequency of the phase angle difference between cart and pendulum phase positions) were also created. Preprocessing of data for each trial was visually inspected for adequate sine wave fit and classification of in-phase or anti-phase patterns in relative phase between the cart and the pendulum.

For each trial, the observed strategy's absolute mutual information, relative (to the mutual information values in the state space that represented the majority of the observed data) mutual information, as well as distance to the global and local maxima, were calculated based on best-fit model-generated position and velocity vectors, as well as model-generated parameter state space. Two repeated-measures ANOVAs were used to examine the differences in absolute and relative mutual information between quintiles of trials. For the model building method, a 2 (Maxima: Global or Local) by 5 (Quintile: 1 to 5) repeated-measures ANOVA was used to look for differences in distances to local and global maxima at each quintile. For the movement restriction method, a 2 (Maxima: Global or Local) by 3 (Quintile: 1, 3, and 5) repeated-measures ANOVA was used instead.

We predicted that mutual information (both relative and absolute) of selected strategies would gradually increase to indicate gravitation towards higher mutual information solutions. If participants used the model building method to formulate and improve the predictability of their strategies, then we would expect to see selected strategies approach the maxima of the simplified models generated from inaccurate pendulum weights than to the maximum of the accurate model. Likewise, if participants used the movement restriction method, then we would expect selected strategies approach the maxima of simplified models generated using reduced amplitude than to the maximum of the accurate model.

Results

Trial-level analysis

Three main patterns of relative movements between cart and pendulum were observed in the data, reflecting an in-phase, an anti-phase, and a hybrid relative phase movement pattern.

Figure 2 shows the raw input signal (placement of finger driving the cart) and raw output signal (phase position of pendulum), basic sine wave fit for raw input signal, Lissajous plot, phase portrait, and distribution of relative phase between input and output signals for a representative trial. Panel A shows the raw input signal overlaid with the raw output signal. An in-phase (where input and output move in tandem) pattern of coordination can be observed. The Lissajous plot in panel C traces changes in position of input and output over time. The observed positive slopes indicate an in-phase pattern. Likewise, a histogram of relative phase between input and output (panel E) shows a similar picture. The phase portrait (panel D) shows that this pattern of coordination was consistent throughout the trial. A standard sine wave function was fitted over the raw input signal to derive an estimate of the observed amplitude and frequency of the input signal (panel B).

In-phase movement patterns accounted for 326 out of 646 trials (50.5%). The average observed amplitude for in-phase trials was 1.84cm. Observed frequency of oscillations was 0.96Hz (with the pacing metronome fixed at 1Hz). The cart pendulum model was successful at generating well-fitted vectors for this pattern of movement in 67.18% of trials. Figure 3 shows the model fit for the representative in-phase trial. A good fit can be observed for each of the four vectors included in the optimization function: cart position, cart velocity, pendulum phase angle, and pendulum phase velocity.

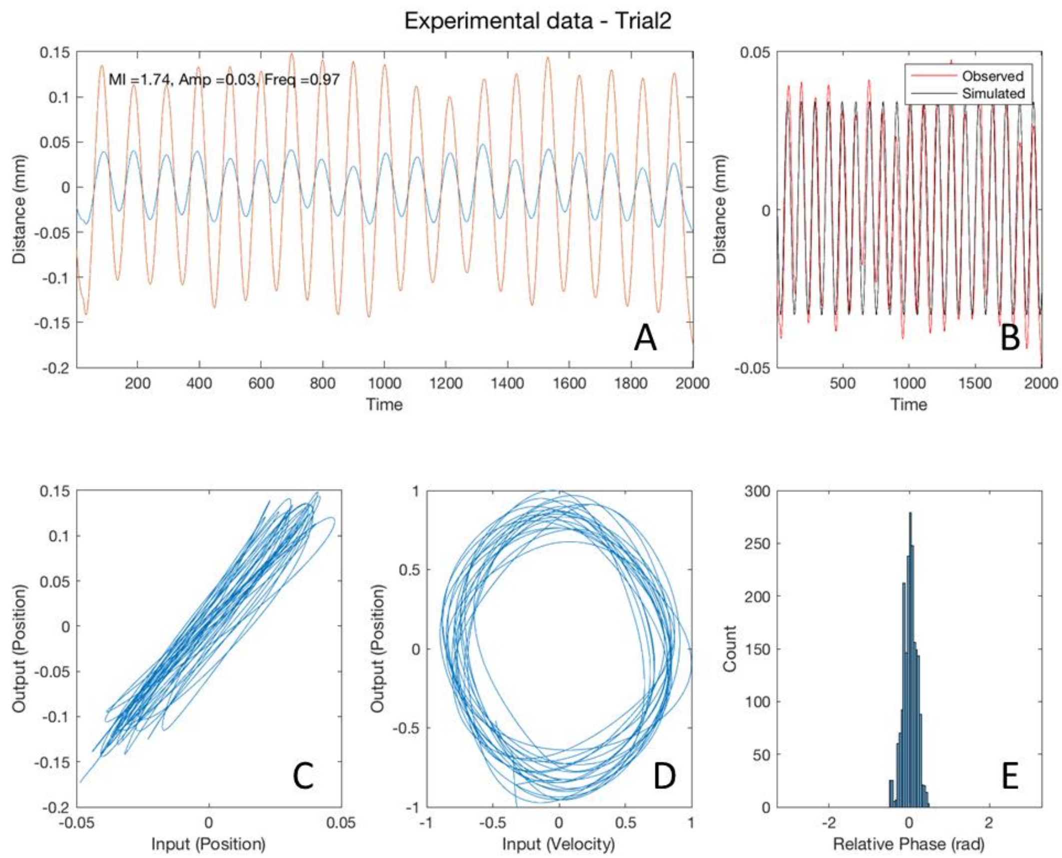

Figure 2. Raw data and preliminary analyses for Participant 5, Trial 2. (A) Raw data of the input signal (finger position - blue) and output signal (pendulum phase position - red) as a function of time. Includes mutual information (MI) between the two signals, estimated amplitude (in meters), and estimated frequency (in Hz). (B) Sine wave function fit of the input signal, used to estimate amplitude and frequency. (C) Lissajous plot showing relative deviations from the means of the input and output signals. (D) Phase portrait of the system, showing input velocity and output position. (E) Histogram of calculated relative phase at each time point in radians.

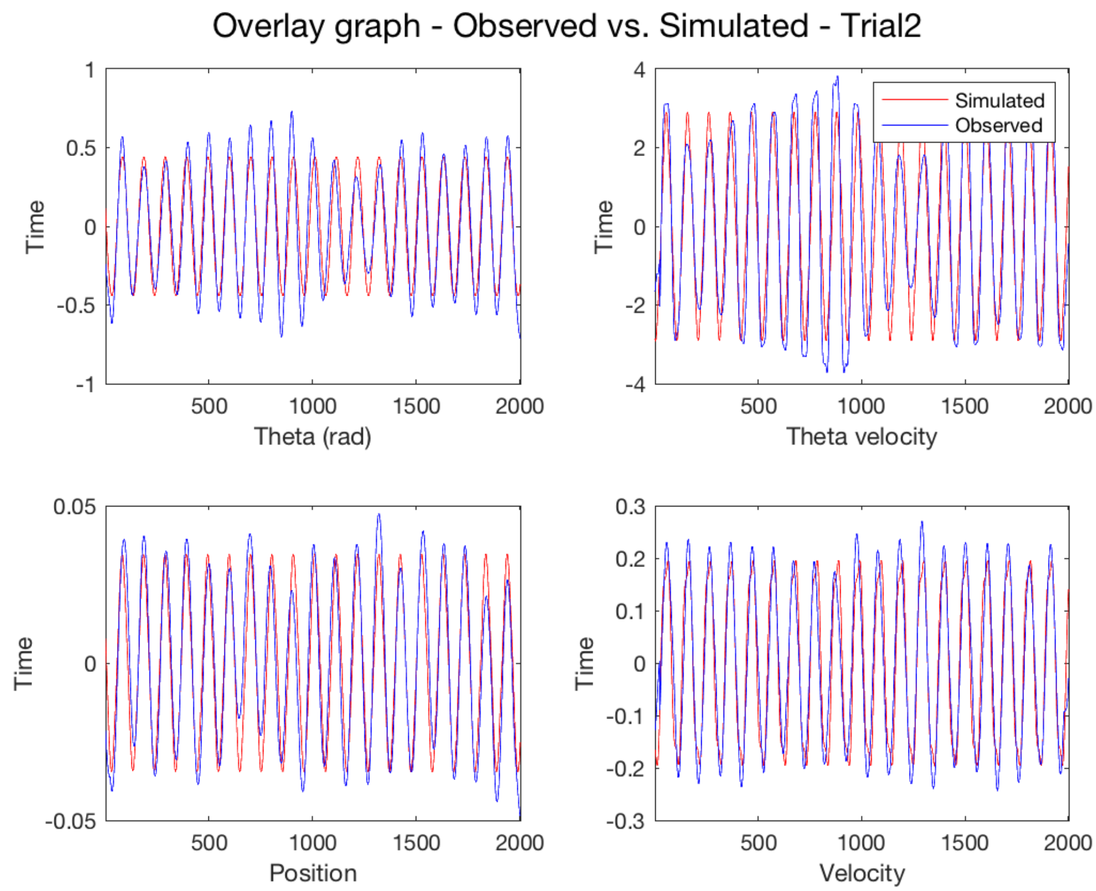

Figure 3. Model predicted output (theta), output velocity, input, input velocity signals overlaid with associated observed signals for participant 5, trial 2.

Figure 4 shows the data for a representative anti-phase trial. Here we observed a movement pattern where the cart moved in the opposite direction to the pendulum. We saw a different pattern in the Lissajous plot, where an increase in position in one vector was accompanied by a decrease in position in the other vector. The relative phase analysis confirmed this assessment by showing relative phase between the cart and the pendulum clustering around $\pm \pi$, or ± 180 degrees.

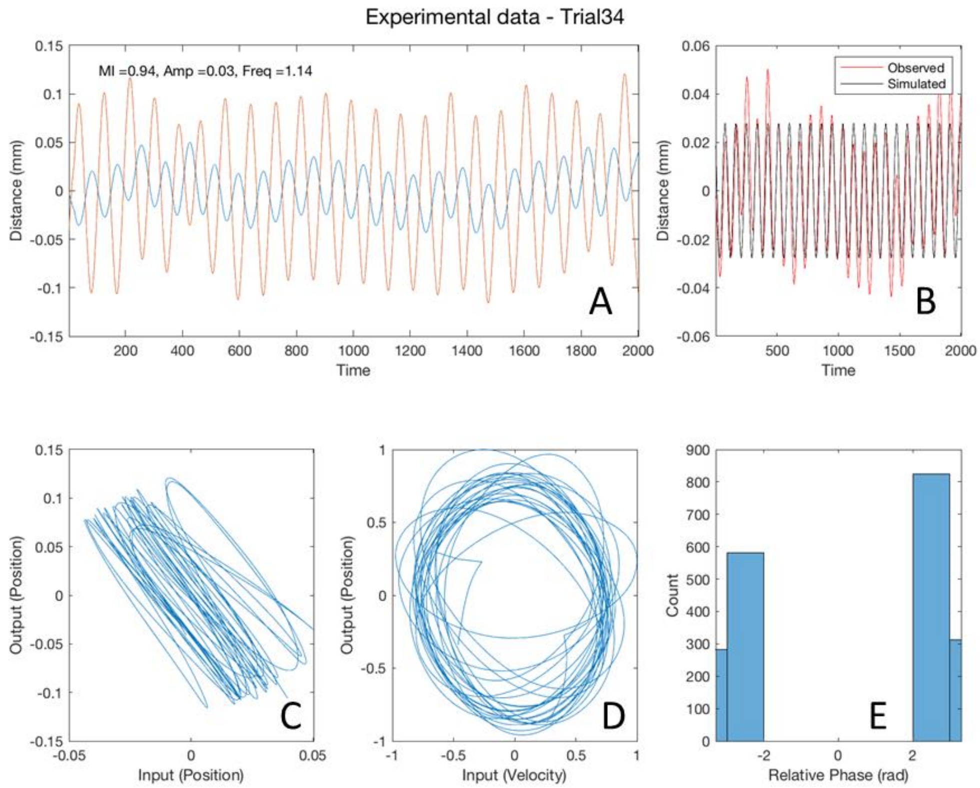

Figure 4. Raw data signals (A) for the input (blue) and output (red) of participant 14, trial 34, with sine wave function fit for the input (B), Lissajous plot (C), phase portrait (D), and relative phase histogram (E).

Anti-phase patterns were uncommon, appearing in 12 out of 646 (1.9%) trials. Since the antiphase strategy requires higher speed and has lower stability (Amazeen, Amazeen, & Turvey, 1998), we did not expect participants to adopt this strategy despite having the option. The observed average amplitude and frequency were 0.0215 meters and 1.12Hz, respectively. The cart pendulum model was able to provide a good fit for observed anti-phase data in 41.46% of the trials. Figure 5 showed a good model fit for the representative antiphase data.

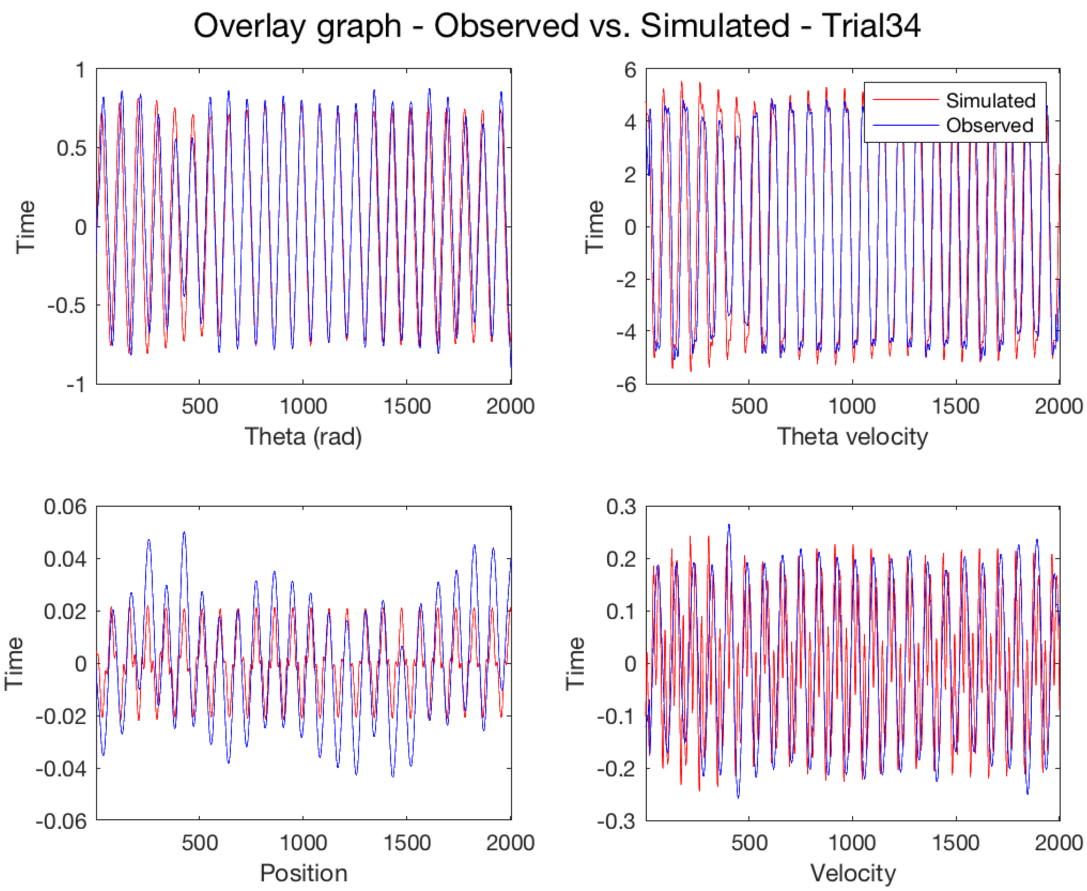

Figure 5. Model predicted output (theta), output velocity, input, input velocity signals overlaid with associated observed signals for participant 14, trial 34.

Figure 6 shows the data for a representative trial exhibiting hybrid movement pattern. This movement pattern was distinct from the in-phase and antiphase pattern in that the cart and pendulum did not move in tandem or in opposite directions. Rather, the peak position of the cart coincided with the neutral position of the pendulum and vice versa. The Lissajous plot showed the participant alternating between in-phase and antiphase segments. The relative phase analysis revealed a similar result, showing relative phase in between in-phase and antiphase.

The hybrid pattern of movement accounted for 308 out of 646 trials (47.7%). The observed average amplitude and frequency were 0.018 meters and 1.02Hz, respectively. The cart pendulum model had difficulty fitting this pattern of movement, producing well-fitted vectors in only 14.94% of trials. Figure 7 shows an example of a poor fit of the hybrid movement pattern. Since hybrid trials made up a substantial number of trials in our data, we attempted several methods to improve model fit (see Appendix I) with inconclusive results. For the remainder of the analyses, we will only use trials where the model was able to produce a good fit.

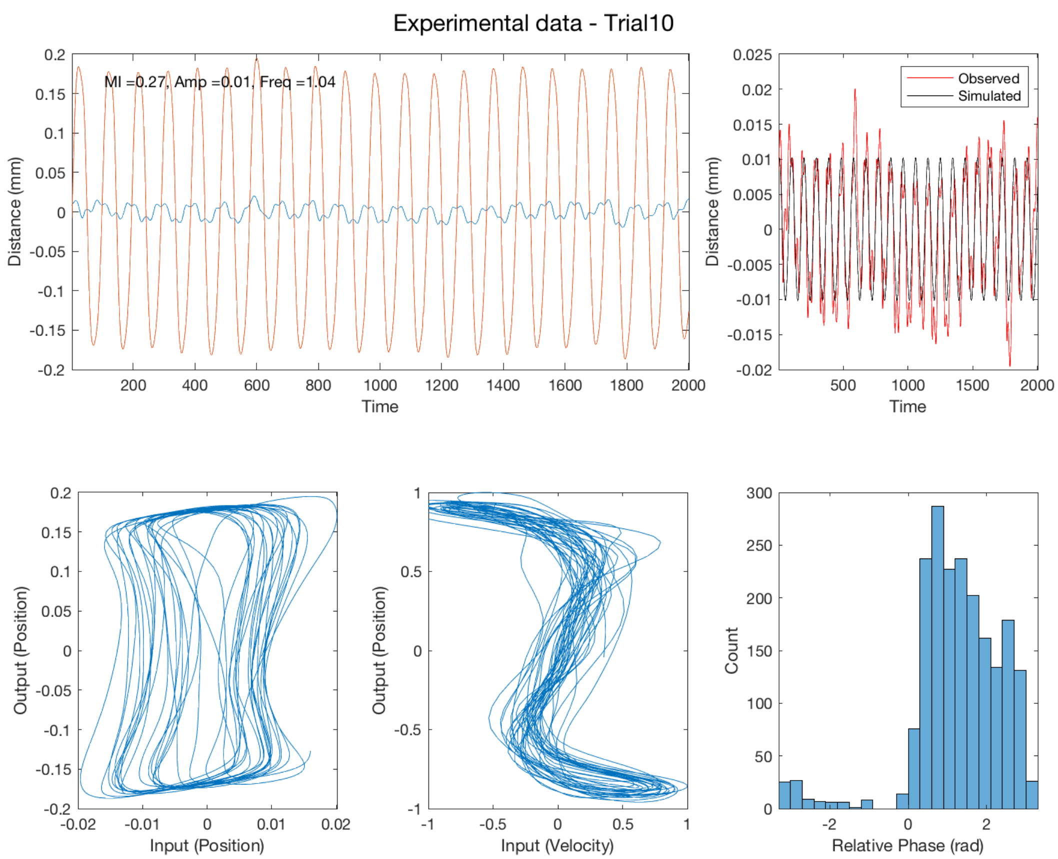

Figure 6. Raw data signals (A) for the input (blue) and output (red) of participant 3 trial 10, with sine wave function fit for the input (B), Lissajous plot (C), phase portrait (D), and relative phase histogram (E).

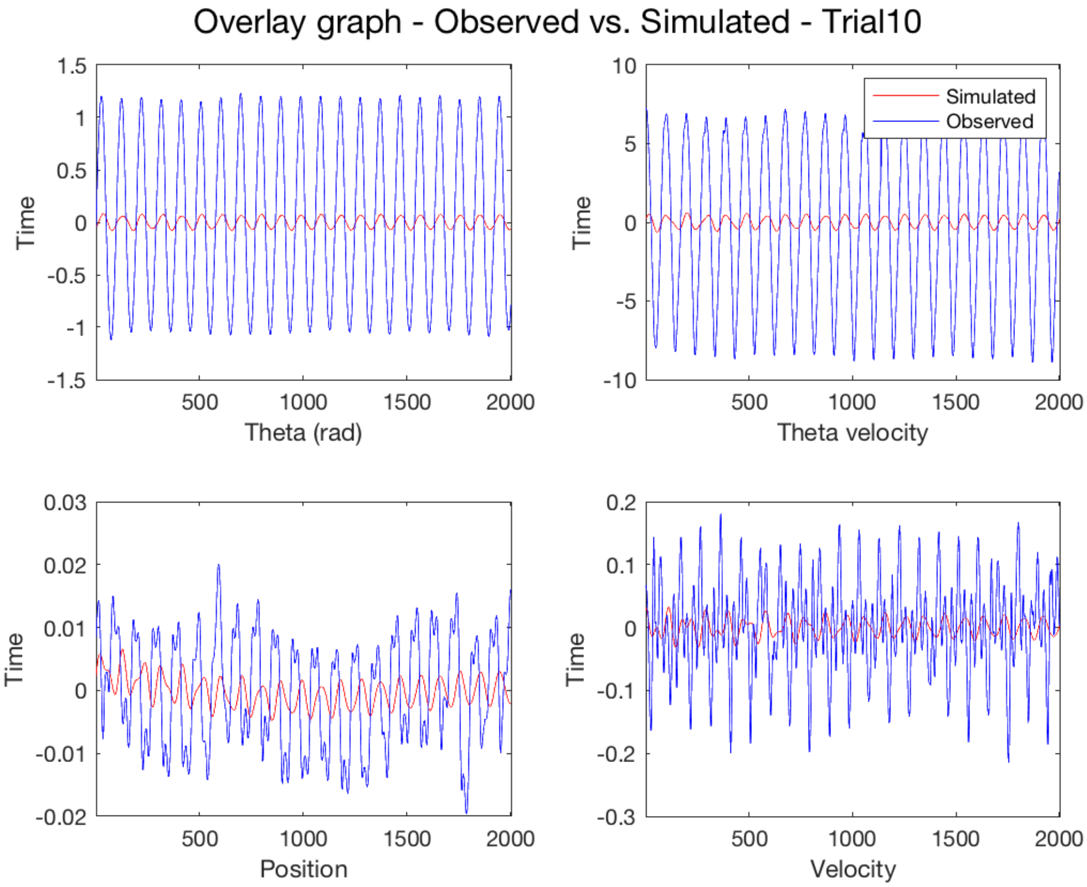

Figure 7. Model predicted output, output velocity, input, input velocity signals overlaid with associated observed signals for participant 3, trial 10. Note that the cart pendulum model was unable to generate a good fit that matched the observed movement pattern.

Parameter state space analysis

For the model building method, we created five parameter state spaces, each corresponding to a different weight level (see Figure 1). For each trial, the estimated K and B parameters associated with their observed movement were used as coordinates.

The coordinates from the first quintile (10 out of 50) of trials were averaged and mapped onto the parameter state space with lowest weight. This process was repeated, with subsequent quintile of trials mapped onto state spaces with successively higher weight. Figure 8 shows the location of each participant's quintile averaged movement strategy, mapped onto the appropriate level of model complexity (with panel A being the simplest model at m_p = 0). Additionally, we mapped the average location of all observed movement strategies in each quantile across all participants to represent the overall chosen movement pattern. The location of the local maximum was also indicated on each parameter state space.

We hypothesized that if participants utilized the model building method, we would see selected strategies adhering closely to the maxima from each simplified model (magenta) instead of the global maximum. Visual inspection revealed that the distribution of chosen strategies did not always line up well with regions of high mutual information (brighter yellow color, see panel B and C). Despite clear changes in the size and shape of regions with high mutual information solutions, there was no clear shift in the distribution of chosen strategies over quintiles. This was apparent in the shift of local maxima (magenta points) and the relatively static positioning of averaged chosen strategies in each quintile.

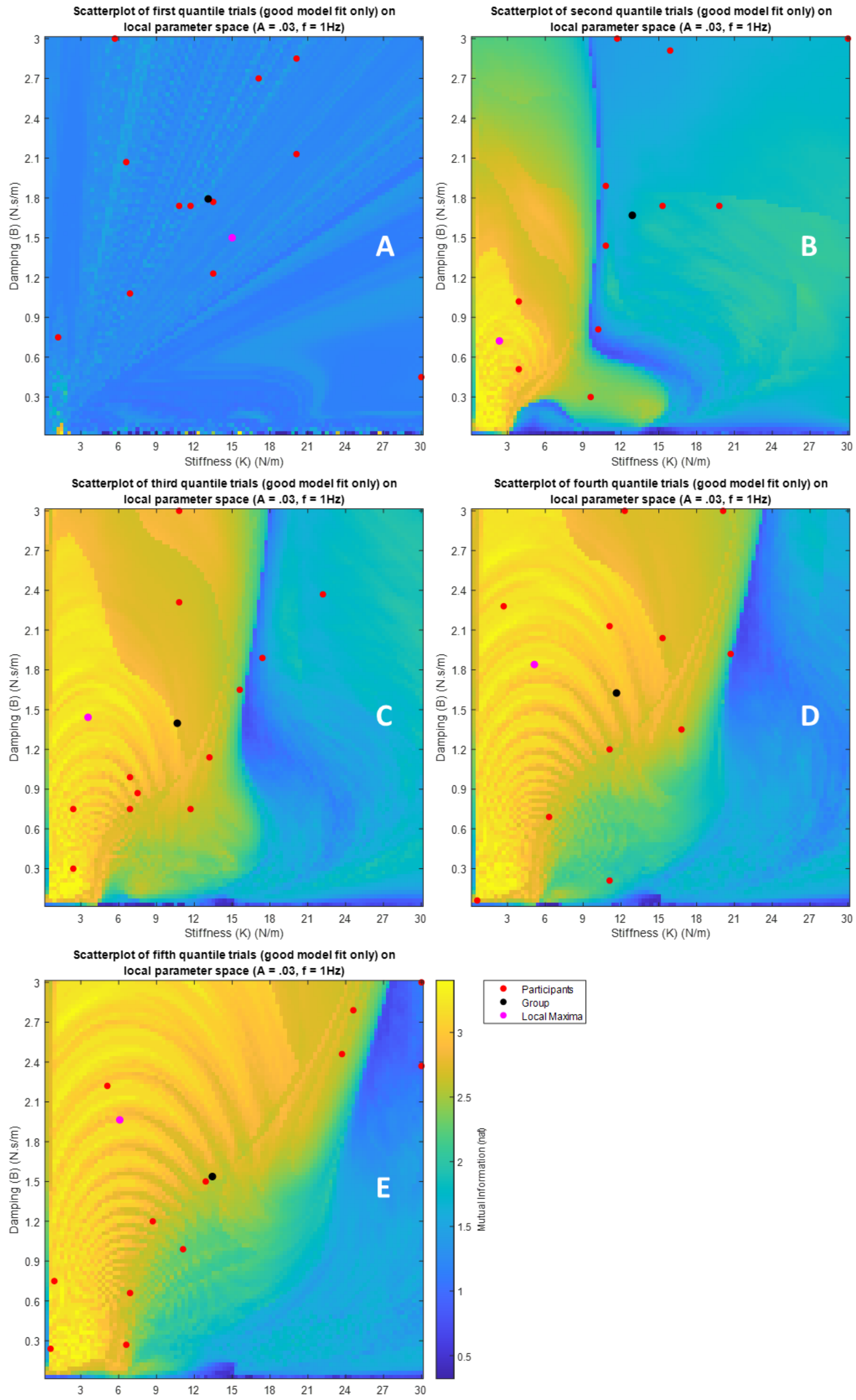

Figure 8. Parameter state space showing mutual information at different values of K, B, and m_p. Panels showing mutual information field at m_p = 0 (A), 0.012 (B), 0.023 (C), 0.035 (D), and 0.046 (E, actual weight). Red dots represent each participant's chosen

strategy, averaged over 10 trials (one quintile). Black dots represent the average strategy across all participants in a given quintile. Magenta dots represent the center of regions with highest mutual information (all points with mutual information above 75th percentile).

For the movement restriction method, we observed that movement amplitude increased over trials for some participants (see Figure 9). We generated the parameter state spaces at 3 movement amplitudes, A = 0.01, 0.02, and 0.03. Similar to our analysis of reduced pendulum weight, we mapped each participants' averaged strategy over the first quintile onto the state space of the lowest amplitude. For A = 0.02, we used participants' strategies in the third quintile. For A = 0.03, we used participants' strategies in the fifth quintile. Average strategy across participants and location of local maximum were also mapped onto each state spaces. Figure 10 shows these parameter state spaces.

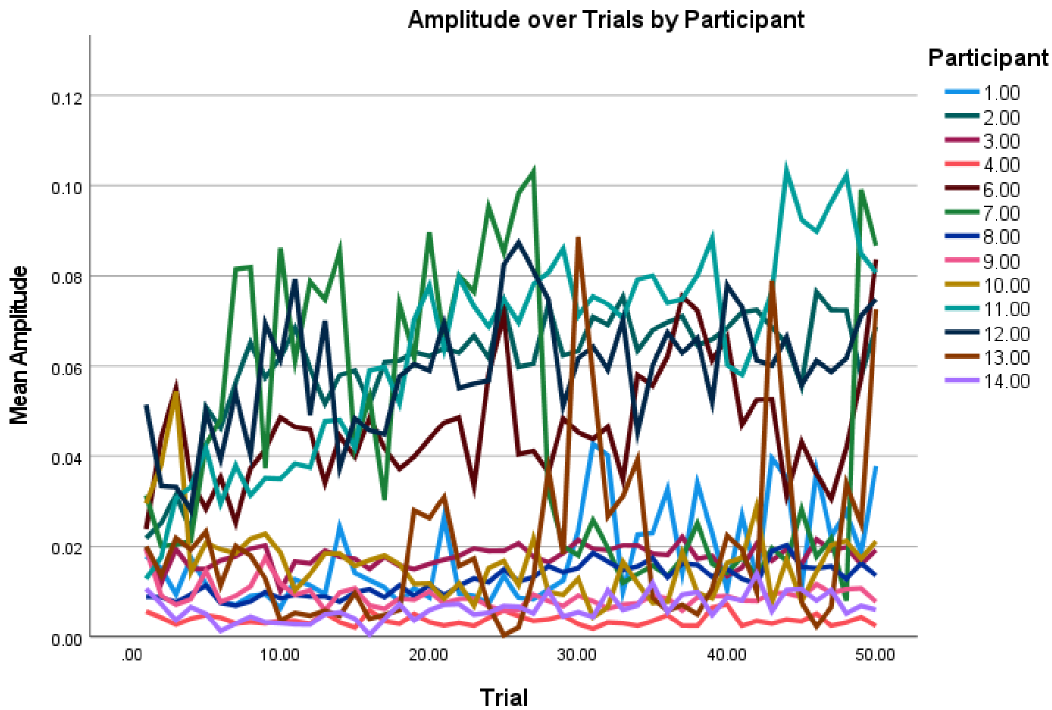

Figure 9. Line graph showing estimated movement amplitudes for each participant over trials.

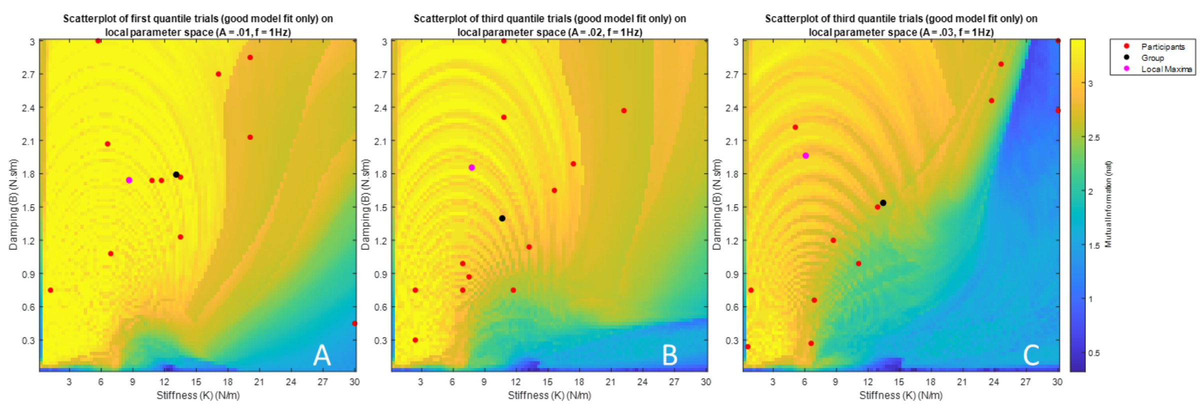

Figure 10. Parameter state space showing mutual information at different values of K, B, and amplitude A. Panels showing mutual information field at A = 0.01 (A), 0.02 (B), 0.03 (C). Red dots represent each participant's chosen strategy, averaged over 10 trials (one

quintile). Black dots represent the average strategy across all participants in a given quintile. Magenta dots represent the center of regions with highest mutual information (above 75th percentile).

We hypothesized that if participants used the movement restriction method, we would see selected strategies adhering closely to the maxima from the simplified models instead of to the global maximum. Visual inspection of the parameter state spaces showed that participants' selected strategies conformed well to regions of high predictability in these simplified models.

As an additional analysis, we mapped each participants' chosen strategies in the first and fifth quantiles onto the full model parameter state space to visualize the evolution of their strategies over time. This analysis resembles the analysis done by Nasseroleslami, Hasson, and Sternad (2014), but with a different set of parameters. Figure 11 shows the resulting quiver plot. We predicted that the mutual information of selected strategies would increase over trials, indicating participants' gradual attunement to solutions with higher predictability. Here, we could see that the majority of participants moved from a region with relatively low mutual information to a region with higher mutual information. This indicated that their chosen strategies exhibited higher predictability over time.

Overall, visual inspection of the parameter state spaces showed substantial shift in the landscape of possible control strategies due to modifications of the model from using reduced pendulum weights (for the model building method) and from using reduced amplitudes (for the movement restriction method). We found that participants' selected strategies seemed to conform more closely to regions of high mutual information, according to simplified models from the movement restriction method. We did not observe a clear clustering of selected strategies around each local quintile maximum for both methods.

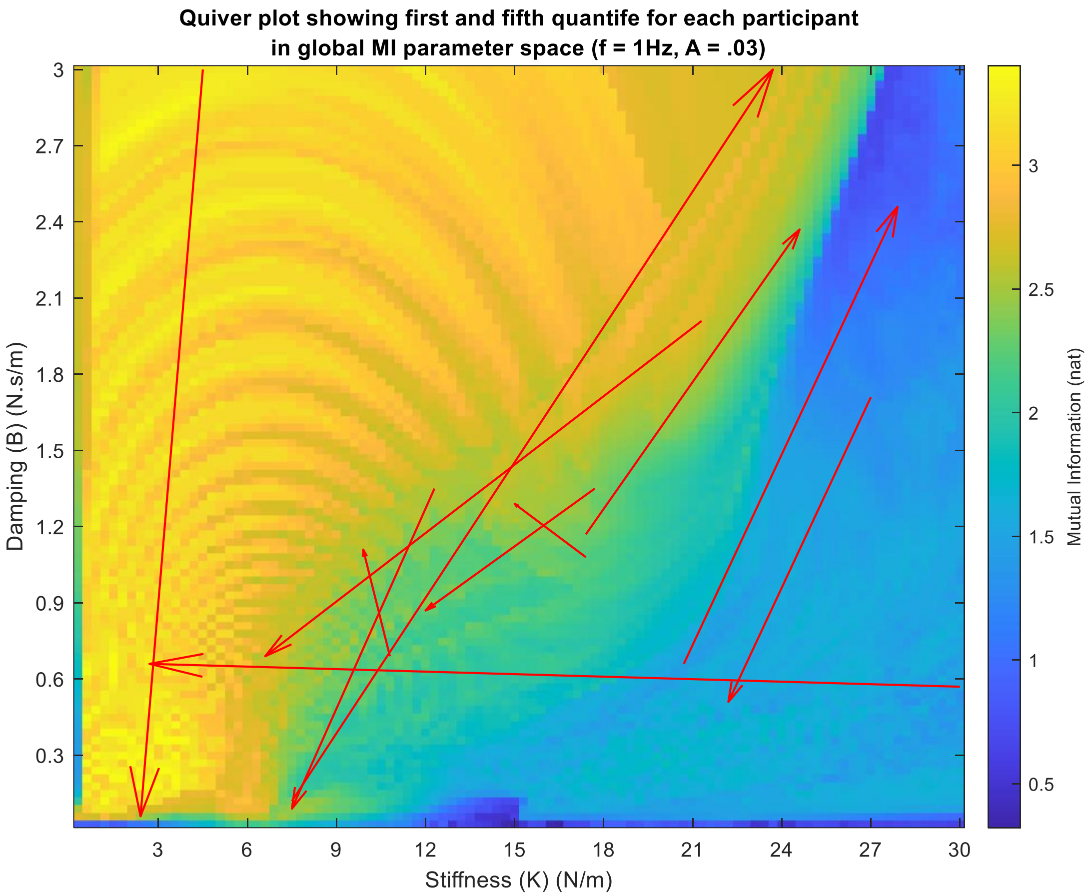

Figure 11. Quiver plot showing each participant's average strategy during the first quintile of trials (beginning of arrows) and the fifth quintile of trials (the end of arrows).

Group-level analysis

We calculated relative mutual information between the cart and the pendulum in each trial as the value found at the associated K/B coordinates in the parameter state space that represented the majority of observed data (f = 1Hz, A = 0.03m, m_p = 0.046kg). In contrast, absolute mutual information was calculated based on estimated parameters specific to each trial. Distances to local and global maxima were only calculated based on distance in the shared parameter state space.

Two repeated-measures ANOVAs were used to examine the differences in absolute and relative mutual information between quintiles of trials. For absolute mutual information, the results showed a significant effect of Quantile, F (4,44) = 6.40, p < .001. A significant linear trend was also found, F (1,11) = 7.37, p = .02. Post hoc analysis indicated that absolute mutual information at the first and second quintiles were both significantly lower than that at the third, fourth, and fifth quintiles, while absolute mutual information of the third, fourth, and fifth quintiles were all similar to each other. Absolute mutual information increased linearly over quintiles, especially the first 30 trials. Figure 12 shows the mean absolute mutual information for each quintile.

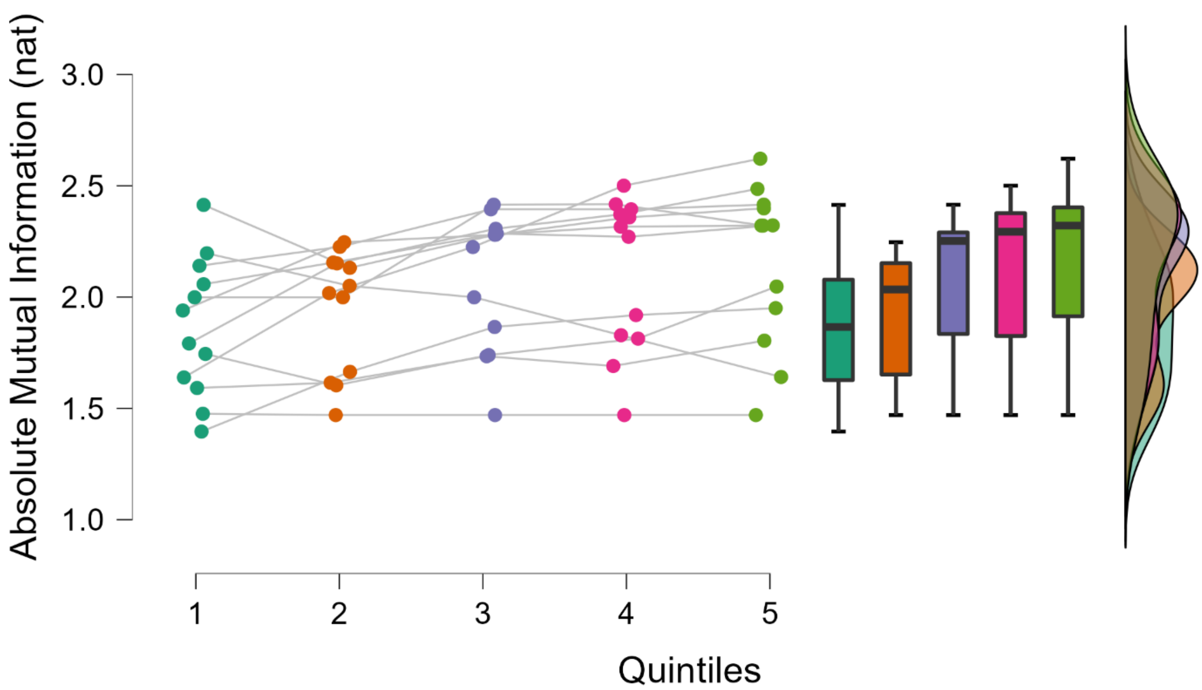

Figure 12. Raincloud plot showing absolute mutual information for each quintile and each participant, as well as aggregated means across participants.

For relative mutual information, the ANOVA test showed no significant effect of Quintiles, F (4,32) = 0.48, p = .750. Participants' quintile-averaged relative mutual information did not significantly change over quintiles. Figure 13 shows relative mutual information for each quintile.

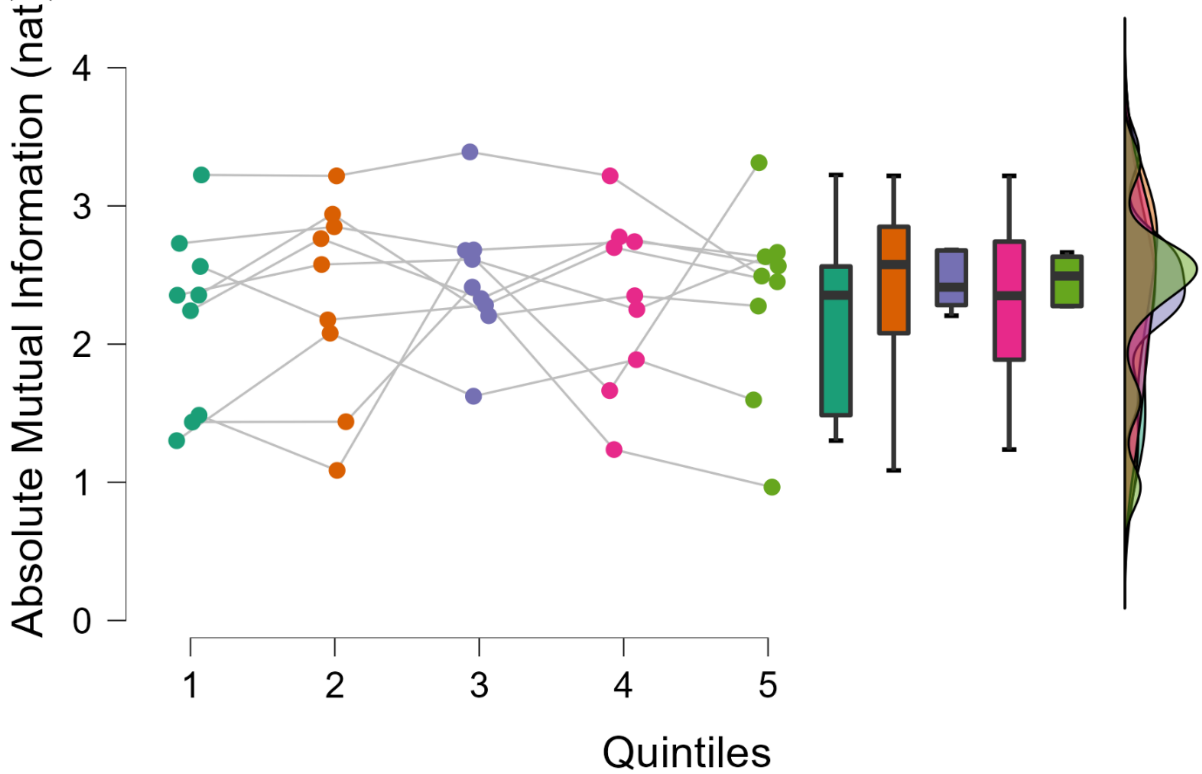

Figure 13. Raincloud plot showing relative mutual information for each quintile and each participant, as well as aggregated means across participants.

We hypothesized that relative and absolute mutual information would linearly increase over quintiles, reflecting participants gravitating towards control strategies with higher predictability over time. The results indicated that participants consistently gravitated over time towards control strategies that had higher predictability, as indicated by the linear and significant increase in absolute mutual information over quintiles.

Next, we looked at data for the model building method. We compared the distance between participants' selected strategies to the maxima of the simplified models versus the distance to the global maximum using a 2 (Maxima: Global or Local) by 5 (Quintile: 1 to 5) repeated-measures ANOVA. The results showed no significant main effect of Quintiles on distance to maxima, F (4,32) = .84, p = .508. There was also no significant main effect of Maxima, F (1,8) = 3.97, p = .081. Marginal means suggested a trend towards lower distance to the local maxima (M = 48.02, SD = 3.61) than to the global maxima (M = 52.29, SD = 3.61). There was a significant interaction effect between Maxima and Quintile, F (4,32) = 2.95, p = .035. However, post hoc analysis revealed that the only significant pairwise difference was distance to local versus distance to global maxima in the first quantile (p = .020). Figure 14 shows distance to global versus local maxima per quantiles.

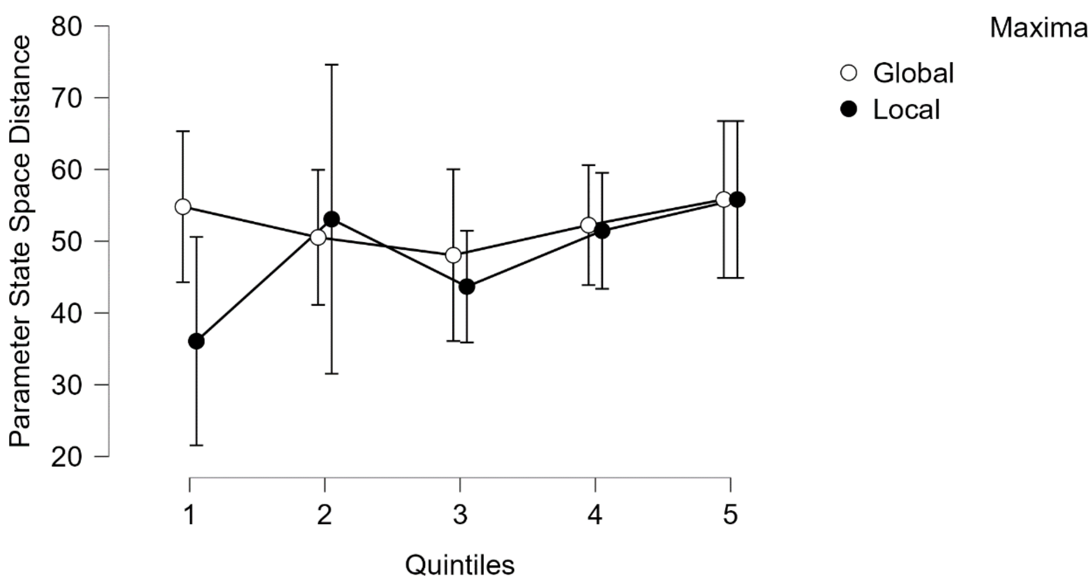

Figure 14. Line plot showing distance to local and global maxima per quantile.

We hypothesized that if participants used the model building method, we would see shorter distance to the simplified maxima than to the global maximum, representing participants choosing strategies using simplified models rather than the accurate model of the system. However, the results showed no difference between the distance from participants' selected strategies to the simplified maxima and to the global maxima, which suggested that the maxima of simplified models did not influence participants' selection of control strategies.

Finally, we looked at the data for the movement restriction method. A 2 (Maxima) x 3 (Quintiles) repeated measures ANOVA was used to examine the differences between distance of chosen strategies to the simplified maxima and distance of chosen strategies to the global maximum. The results showed no significant main effect of Quintiles, F (2, 20) = 1.92, p = .172. However, we found a significant main effect of Maxima, F (1,10) = 39.87, p < .001. Distance to the simplified maxima (M = 46.94, SD = 11.32) was significantly lower than distance to global maximum (M = 51.31, SD = 11.32). The interaction between Quintiles and Maxima was also significant, F (2,20) = 17.42, p < .001. Post hoc test indicated that the differences between local and global maxima in the first and third quintiles were both significant (all p < .001), whereas this difference was not significant in the fifth quintile (see Figure 15).

We hypothesized that if participants used the movement restriction method, we would see shorter distance between participants' selected strategies and the simplified maxima, compared to the global maximum. The results showed significantly shorter distance between selected strategies and simplified maxima, which suggested that participants were relying on movement restriction to simplify the complexity of the system and find solutions with higher predictability. This result was also consistent with our observations of participants using lower amplitude during early trials of the experiment.

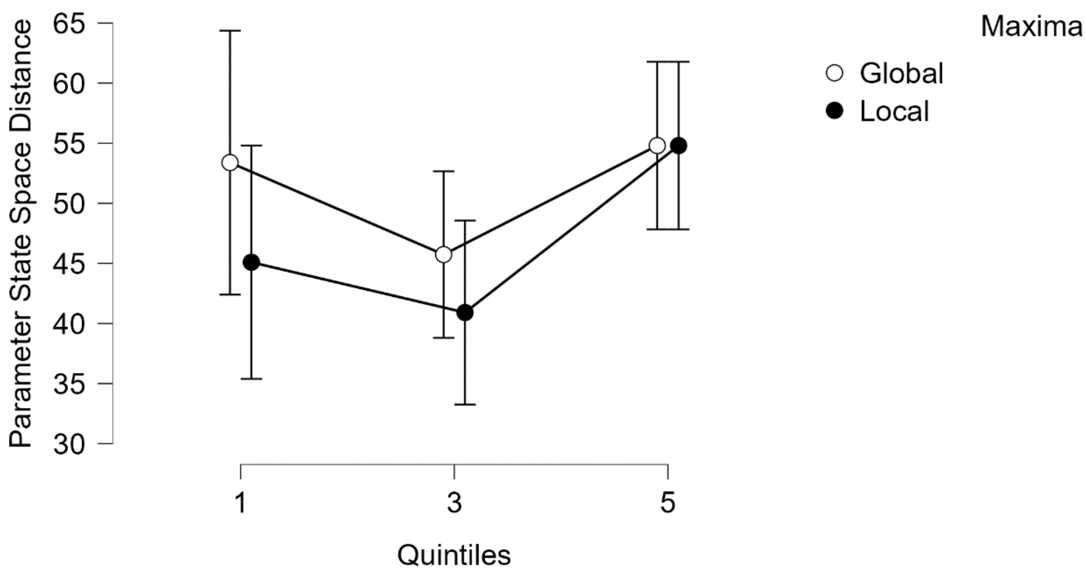

Figure 15. Line graph showing mean distance to local (adjusted with movement amplitude) maxima versus distance to global maximum over quintiles and model complexity.

Discussion

In this first experiment, we extended recent findings suggesting predictability as the primary control policy when interacting with complex, nonlinear tool systems. Our contribution focused on the method with which participants generated and optimized control strategies for higher predictability. Recent findings revealed that people prioritized and gravitated towards solutions with higher predictability when interacting with complex tool systems (Wallace, Kong, Rodriguez, & Lai, 2021; Maurice, Hogan, &

Sternad, 2018; Bazzi & Sternad, 2020). How do people continually adjust control strategies to arrive at higher predictability solutions, especially during early interactions, when information about the system is limited? We focused our investigation on two methods. The first method, based on the reasoning-based and manipulation-based theories of tool use (Osiurak et al., 2010; Goldenberg, 2013; Bauxbaum, 2001), had participants estimate the physical measurements of the system, then use this information to construct an accurate model that can be used to simulate better control strategies. The second method, based on dynamical systems theory (Bernstein, 1967; Newell & Vaillancourt, 2001), had participants restrict their movements during initial interactions to observe the system's dynamics, then gradually adjust their control strategy until the predictability between their input and the system's output improves. To test whether participants employed one of these methods, we generated a series of simplified models based on each method, then compared participants' selected strategies against the model predicted strategies with high predictability.

First, our results replicated findings in the literature on control of complex objects. We found that the mutual information between the cart and the pendulum positions gradually increased over trials, indicating that participants were gravitating towards movement strategies that are highly predictable. This finding reinforced the notion that predictability is prioritized in selection of control strategies when interacting with complex objects (Maurice et al., 2018, Bazzi & Sternad, 2020).

Second, we found that simplified models created by simulating lower pendulum weight did not accurately describe the evolution of participants' chosen strategies over time. This finding did not support centralized control accounts of tool use, which argued that internal models constructed from technical reasoning and functional knowledge are important in action planning and control of tool interactions (Osiurak & Badets, 2016; Goldenberg, 2013). However, it is possible that other methods of model simplification and simulation could more accurately account for participants' observed behavior.

In contrast, we found that simplified models created by reducing movement amplitude, which was utilized by some participants, were able to accurately describe participants' chosen strategies at different stages of attunement with the complex system. This finding supported the dynamical systems approach, which argued for restriction of a peripheral degree of freedom during initial interactions with a novel, complex systems in order to simplify the system and discover its inherent dynamics (Bernstein, 1967; Newell & Vaillancourt, 2001; Mitra et al., 1998). We found that some participants restricted movement amplitude in early trials, and that participants' selection of strategies were consistent with information provided by simplified models of the system that were generated by limiting amplitude. While amplitude is not itself a degree of freedom of the biomechanical system, it can be restricted by an adjacent joint-muscular degree of freedom. A follow up study examining the movement kinematics of arm joints during this task can shed light into how amplitude restriction was implemented. Participants' reliance on simplified models achieved through physical manipulation of the system also aligned with the embodied approach (Martel et al., 2006; Baccarini et al., 2012), which eschewed model-based, centralized control in favor of enacting control at the periphery.

CHAPTER 3

EXPERIMENT 2

In the first Experiment, we demonstrated that the task of forming and optimizing control strategies can be accomplished by adjustments of interaction dynamics at the biomechanical periphery. Our finding showed that the principle of predictability still holds when information about the system is missing. In Experiment 2, we examined the role of predictability in controlling complex objects when there was a change in task goal or action intention.

Intention occupied a prominent place in many theories of perception and action. Gibson (1979), whose theory contributed to the development of the dynamical systems perspective, described intention (or need in his terminology) as the agent-specific anchor in the perception action link between agent and environment (see also Shaw, Turvey, & Mace, 1982). Subsequent authors in the dynamical systems approach framed intention as contextual constraints on system dynamics (Newell, 2003; Newell & Valvano, 1998). However, this view was disputed. For example, Thill et al. (2013) argued that context should be limited to external factors that do not explicitly influence behavior (such as the presence of a distractor) whereas intention should be viewed as an internal representational state. In accordance with this view, centralized control theories on tool use likewise described intention as an internalized state against which action plans can be compared, filtered, or evaluated (Buxbaum, 2001; Borghi, 2004; Osiurak, 2013; Osiurak et al., 2016).

Authors from both perspectives agreed that intention can influence motor behaviors. For example, Shaw et al. (1982) described a bench as sittable when the agent's intention was to find a place to rest. However, the same bench could be perceived as jumpable if the intention was to escape a threat. Rosenbaum et al. (1990) showed that people would use an awkward grip to transport an object because they intended to end the movement in a comfortable posture. Tipper et al. (2006) showed that people were faster to respond to a right-facing door handle with the right hand if the handle was depressed (i.e., active or with an action intention) than when the handle was at a neutral position (i.e., passive or without an action intention). Similarly, Costantini et al. (2010) found that people were faster to respond to the orientation of the handle on a mug if the mug was within reach (actionable), but not when the mug was out of reach (not actionable).

In modeling, intention can be instantiated as either the objective function or as a bounded range on a model parameter (Schaal et al., 2007). For example, in the cart-pendulum model, the intention to control the system without making mistakes was translated into an objective function that maximized predictability. Similarly, the minimum movement constraint was translated into a range of K and B values that produced excessively small oscillations, thus failing the task requirement. It is important to note that in the latter instance, nothing about the inherent dynamics of the cart-pendulum system prevented a participant from executing a strategy that fails to meet the requirement. Rather, the restriction was translated from a verbal instruction into a system constraint, which participants used to reject control strategies during interactions with the complex object. To what extent can such constraints bias the selection of execution strategy? Are there instances where the principle of maximizing predictability is ignored in favor of other intentional goals? We examined these questions in the context of synchronization patterns between input and output of the cart-pendulum system.

Synchronization is a common feature in many nonlinear dynamical systems, especially when coordination between components is the focus. The concept can be traced back to von Holst’s (1973) study on the coordination between fins of the Labrus fish, to Kelso’s (1984) on bimanual coordination (also Haken, Kelso, & Bunz, 1985), to coordination among team members (Gorman, Amazeen, & Cooke, 2010; Gorman, Cooke, Amazeen, & Fouse, 2012), as well as numerous physical, physiological, and chemical systems (Wallace et. al., 2021). Studies on synchronization often focus on nonlinear transitions between qualitatively distinct states. For instance, Maurice et. al. (2018) found two clusters of strategies in data of participants interaction with the cart-pendulum system: a low-frequency strategy cluster, and a high-frequency strategy cluster. In the low frequency category, the relative phase between the cart position and the pendulum position stayed close to 0 degree, indicating in-phase synchronization. In the high-frequency group, the relative phase stabilized to 180 degrees, indicating anti-phase synchronization. High frequency strategies were also found to require significantly more energy to execute. In a follow-up study, Wallace et. al. (2021) found that both strategies were stable, and that transitions between these synchronous states could happen abruptly near the resonant frequency of the system.

Observing behavior at this equilibrium point allows us to tease apart the effect of action intention on the selection of strategy in complex object control. Based on previous findings on the effects of action intention, we hypothesize that intention, in the form of a speed incentive, can bias subjects into more active exploration of the state space and higher likelihood of selecting energy-demanding strategies. However, this bias would not interfere with the predictability principle, since losing control of the system would also result in negative performance. That is, we predict that a change in intention would induce participants to shift from the slow but highly predictable in-phase pattern to the speedy but less predictable antiphase or hybrid patterns. This shift would be reflected in the parameter state space as closer clustering of selected strategies around region of antiphase solutions compared to the distribution of selected strategies in Experiment 1, when no speed incentive was imposed. However, participants would still adhere to the predictability principle and avoid unstable (chaotic) movement patterns.

Methods

Participants

A total of 21 human subjects were recruited from the Introductory Psychology student pool at Arizona State University to participate in the experiment. One subject failed to follow instructions and was removed from the data, resulting in a total sample size of N = 20.

Apparatus

The apparatus used for Experiment 2 was identical to that of Experiment 1. A cart (m_c = 20 g) was placed on a suspended single-rail track. The track restricted the cart's movements to approximately 20cm in both lateral directions (with clearance on both sides). Suspended from the cart was a pendulum (m_p = 46 g) connected via wire of length 0.19 m. Movements of the cart and pendulum were tracked via two infrared-emitting diodes, with an Optotrak 3020 motion-capture camera recording movements at a sampling rate of 100Hz.

Procedure

The procedure for Experiment 2 was similar to that of Experiment 1. Participants (N = 20) were instructed to use their finger to oscillate a cart-pendulum system at a fixed starting frequency (1Hz). Participants were instructed that they could go faster than the metronome (to facilitate anti-phase strategies), but no slower (to avoid stationary strategies). Each participant performed 50 trials of 45 seconds each, in 5 blocks of 10 trials. However, unlike in Experiment 1, where the instructions were simply to control the system in a comfortable manner, Experiment 2 was framed in the context of an ecologically relevant scenario. Participants were told that they were training to be a server at a restaurant, and that their goal was to learn how to carry drinks to the customers in the most efficient manner. They were told that they would receive a higher score if they moved faster but would receive a penalty if the drink "spilled" (the pendulum went outside the boundary of the target boxes). During the rest periods between blocks, the instructions were repeated to reinforce the effect of the manipulation. After 50 trials, participants provided demographic information. Then they were debriefed and dismissed. Overall, the inherent dynamics of the physical system were the same as that of Experiment 1. However, the action intention of the task had changed to clearly favor high frequency strategy (i.e., anti-phase pattern) even when this was less energy efficient. The experimental procedure was approved by the Institutional Review Board at Arizona State University.

Modeling

We used the same model described in Experiment 1 for Experiment 2. Estimates of K and B parameters that fit an observed movement pattern still represented the chosen strategy for that trial. Model-generated parameter state spaces were similar to those in

Experiment 1. To enable comparison with data from Experiment 1, quantile-averaged movement strategies were mapped onto the same global parameter state space used in Experiment 1 (A = .03m, f = 1Hz). Therefore, the location of the global maximum of mutual information remained unchanged. However, unlike in Experiment 1, instead of calculating local maxima based on different weight or amplitude levels, we calculated a single maximum representing the center of the anti-phase strategy cluster in this Experiment. The location of this maximum was calculated as the average coordinates of all strategies exhibiting anti-phasic movement patterns. The relative phase between the cart and the pendulum in model-generated movement vectors was determined based on the linear regression slope of the Lissajous plot of that movement pattern (negative slope indicated anti-phase relation). Figure 16 showed the location of this maximum against the Lissajous slopes of each K/B parameters pair.

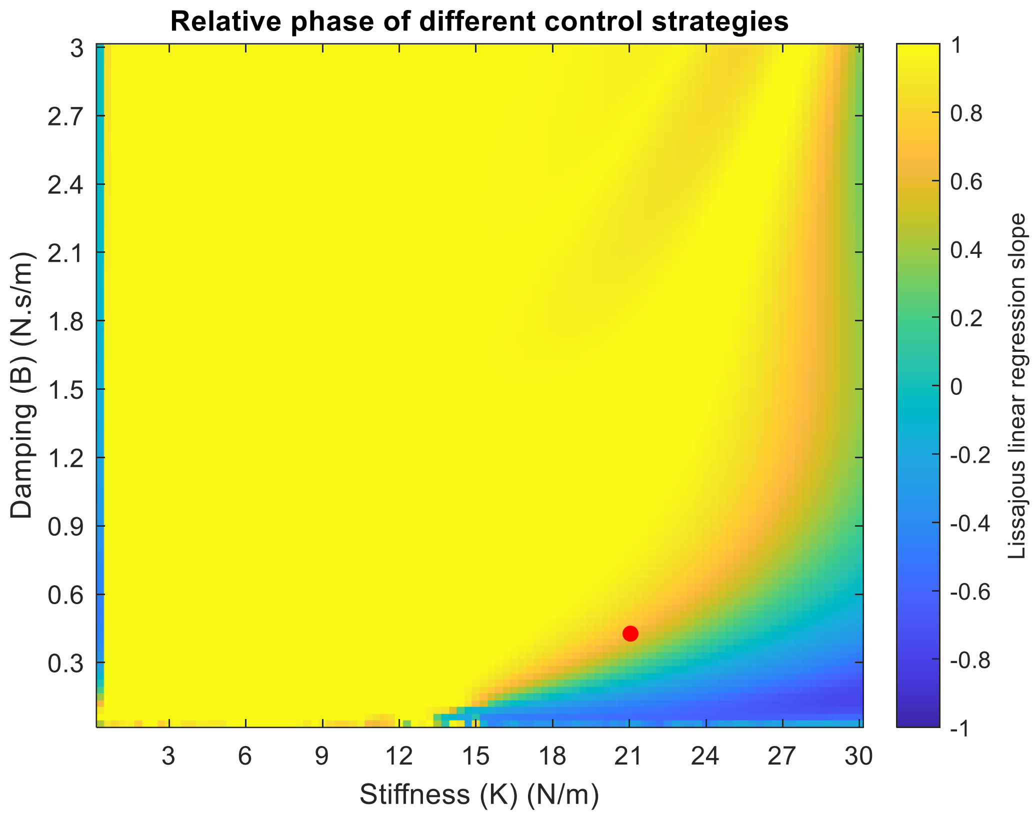

Figure 16. Parameter state space showing the Lissajous linear regression slope for each K/B parameter pair. Red dot indicates the average coordinate of all points with slope below 0.

Data processing and analysis

There was no change to the data processing pipeline in Experiment 2 compared to Experiment 1. For each trial, the observed strategy's absolute mutual information (using the estimated parameters specific to that trial), relative (to the global parameter state space) mutual information, distance to global maximum, and distance to anti-phase maximum were calculated. Looking at just data from Experiment 2, we used two repeated-measures ANOVAs to examine the differences in absolute and relative mutual information between quintiles of trials. Then, a 2 (Maxima: Global or Antiphase) by 5

(Quintile: 1 to 5) repeated-measures ANOVA was used to look for differences in distances to the antiphase maximum and the global maximum at each quintile. Next, we compared results from Experiment 1 and Experiment 2. Four 2 (Experiment) x 5 (Quintiles) ANOVAs were used for each of the four dependent variables: absolute mutual information, relative mutual information, distance to global maximum, and distance to antiphase maximum. These analyses examined whether the change in action intention compelled participants to shift towards more anti-phasic strategies.

We hypothesize that an intentional shift can influence participants' selection of movement strategies, pushing them towards solutions that are more energy-demanding and less (but still highly) predictable. Therefore, we predict that mutual information (both relative and absolute) of selected strategies would gradually increase to indicate gravitation towards higher mutual information solutions. However, because the change in intentional context encourages lower predictability strategies, we predict that this increase would not be as pronounced, and that overall mutual information would be lower compared to results in Experiment 1. Likewise, we predict that selected strategies would be closer to the antiphase maximum and further away from the global maximum for participants from Experiment 2 than for participants from Experiment 1.

Results

Trial-level analysis

Similar to the data in Experiment 1, we found three main patterns of movement in the data: in-phase, antiphase, and hybrid. Refer to Figure 2, 4, and 6, respectively, for examples of these movement patterns. In-phase movement pattern accounted for 244/999 trials, or 23.3%. The average observed amplitude was 4.86cm. The average observed frequency was 0.95Hz. The cart-pendulum model was able to generate a good fit for 80.33% of trials in this category. Antiphase trials accounted for 110/999 trials, or 10.5%. The average observed amplitude was 4.44cm. The average observed frequency was 1.16Hz. The cart-pendulum found a good fit for 53.64% of trials of this type. Finally, the hybrid movement pattern accounted for 645/999 trials, or 61.4%. The average observed amplitude was 0.98cm. The average observed frequency was 1.07Hz. Similar to Experiment 1, the cart-pendulum was only able to generate a good fit for 15.5% of trials of this type. Refer to Appendix I for more information on our treatment of the model to accommodate these trials. For subsequent analyses, only trials with good model fits were included.

We hypothesized that a change in action intention would result in a shift in the selection of control strategies from the in-phase pattern to the antiphase and hybrid patterns. Compared to the distribution of movement patterns in Experiment 1, the trial-level analysis revealed a drastic shift in selected strategies from the in-phase pattern to the antiphase and hybrid patterns. The percentage of trials with the in-phase pattern dropped from 50.5% in Experiment 1 to 23.3%. At the same time, the proportion of trials with antiphase pattern increased to 10.5% (from 1.9% in Experiment 1). Similarly, the proportion of hybrid trials increased to 61.4% (from 47.7% in Experiment 1).

Parameter state space analysis

For each quintile, we mapped the quintile-averaged movement strategies, group averaged movement strategy, location of global maximum, and location of antiphase maximum onto the global parameter state space (K ranging from 0 to 30N/s in 100 intervals, B ranging from 0 to 3 N.s/m in 100 intervals, m_p = 0.046kg, A = 0.03m, f = 1Hz). Figure 17 showed the distribution of these data points in each quintile.

We hypothesized that the inclusion of an action intention would induce participants to select more control strategies in the antiphase region of the parameter state space. Visual inspection of Figure 17 showed no clear shift in participants' movement strategies over trials. However, the distribution of selected strategies seemed more evenly spread, with more strategies being selected in the antiphase regions (green dot), compared to the distribution in Experiment 1.

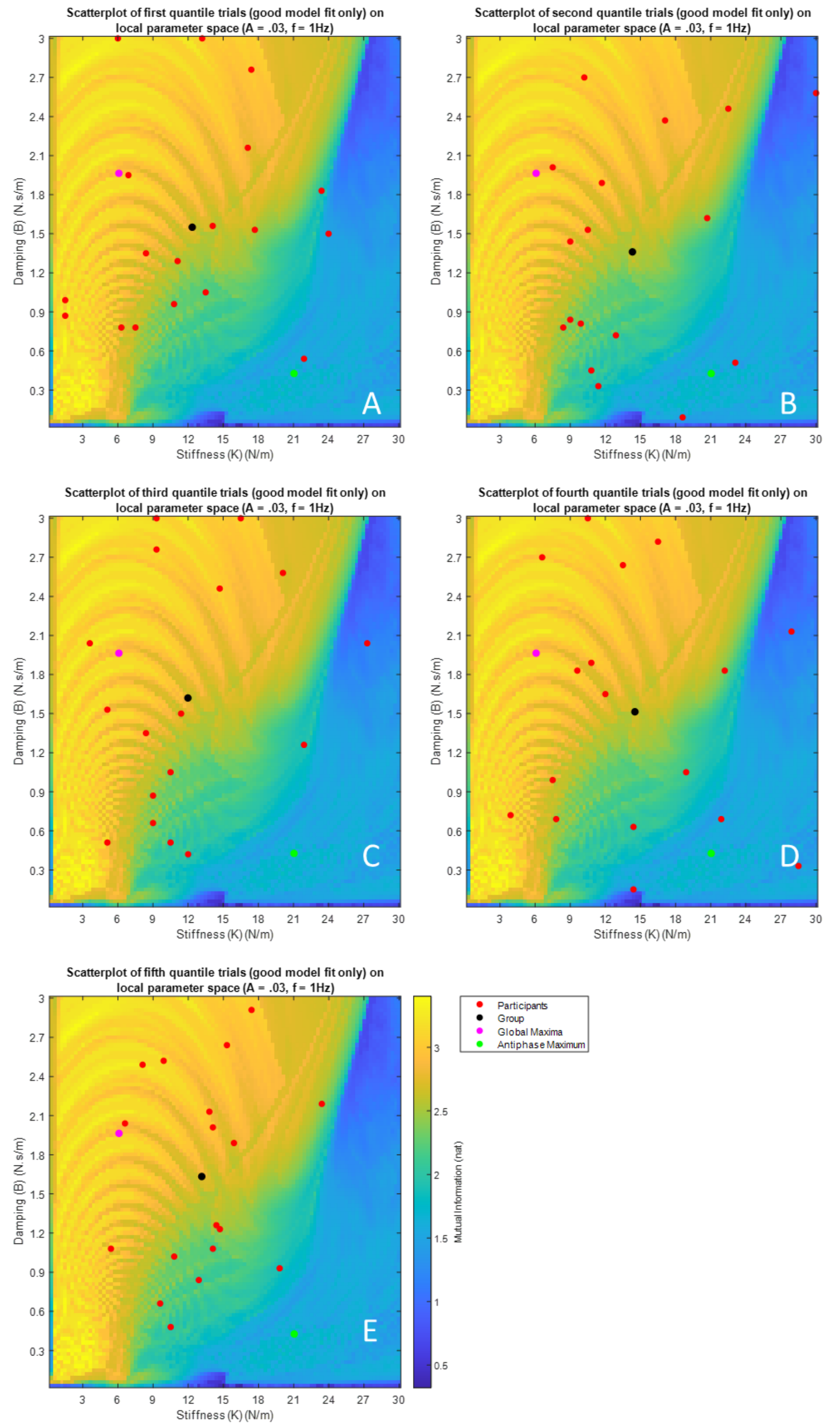

Figure 17. Parameter state space showing mutual information at different values of K and B. Panels showing mutual information field each quintile (A-E ~ 1-5). Red dots represent each participant's chosen strategy, averaged over 10 trials (one quintile). Black dots

represent the average strategy across all participants in a given quintile. Magenta dots represent the center of regions with highest mutual information (above 75th percentile). Green dots represent the antiphase maximum.

Group-level analysis

We first performed a manipulation check to determine whether our intention manipulation had a significant effect on participants' frequency in their trials. This manipulation check was performed on all trials, regardless of model fit. We used a 2 (Experiment) x 50 (Trial) repeated measures ANOVA to look for the effect of Experimental manipulation on observed frequency. The results showed no significant main effects of Trial, F (49,1519) = 1.20, p = .163, or of Experiment, F (1,31) = 4.06, p = .053. There was a significant interaction effect between Trial and Experiment, F (49, 1519) = 2.43, p < .001. Post hoc tests revealed significant differences in frequencies between Experiment 1 and 2 in the late trials (see Figure 18). The intention manipulation in Experiment 2 resulted in significantly higher movement frequencies in late trials compared to Experiment 1.

Looking first at the data from Experiment 2, we examined whether the mutual information of selected strategies exhibited linear increase over trials, as seen in Experiment 1. The repeated-measures ANOVA comparing absolute mutual information between Quintiles was not significant, F (4,68) = 0.19, p = .944. Likewise, the repeated-measures ANOVA looking at differences in relative mutual information between Quintiles was also not significant, F (4, 52) = 0.52, p = .718. In both tests, no main effect of Quintiles was observed, indicating that the mutual information of selected strategies did not increase as a function of trial.

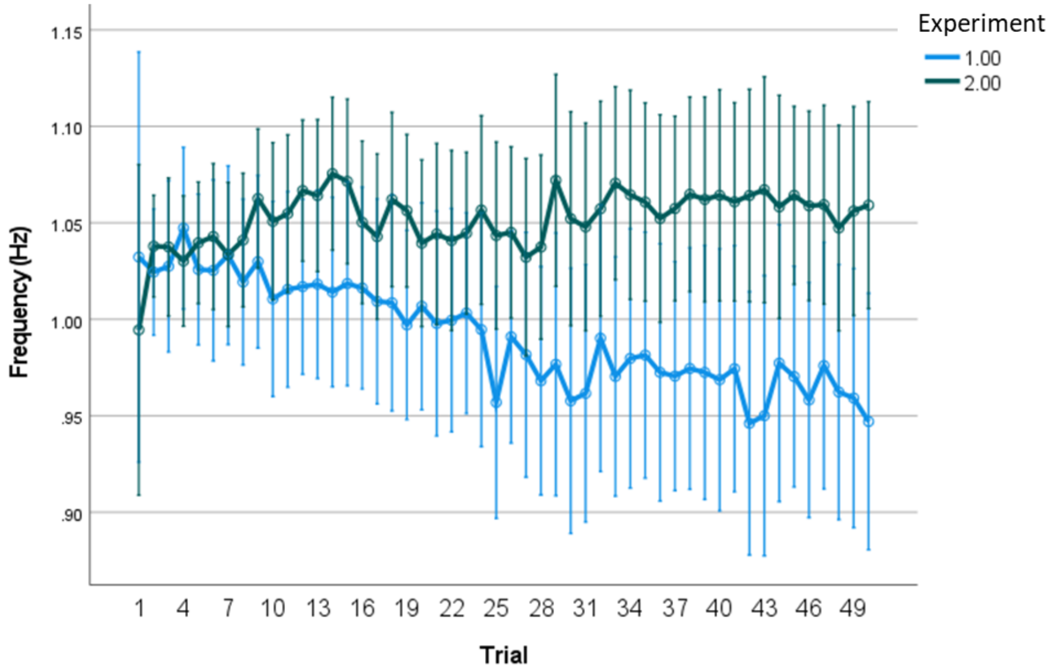

Figure 18. Line graph showing observed frequency in each trial for Experiment 1 and Experiment 2.

Next, we look at the relative differences in distance to the global maximum and to the antiphase maximum over Quintiles. Because the intention manipulation we introduced favored higher frequency strategies, we predicted that the distance between selected strategies and the antiphase maximum would be shorter than distance to the global (in-phase) maximum. The 2 (Maxima) x 5 (Quintiles) ANOVA showed no significant main effect of Maxima, F (1,13) = .83, p = .380, no main effect of Quintiles, F (4,52) = .70, p = .596, and no significant interaction effect, F (4,52) = .83, p = .510 (see Figure 19). Participants selected strategies that were of equal distance from the global maximum and from the antiphase maximum.

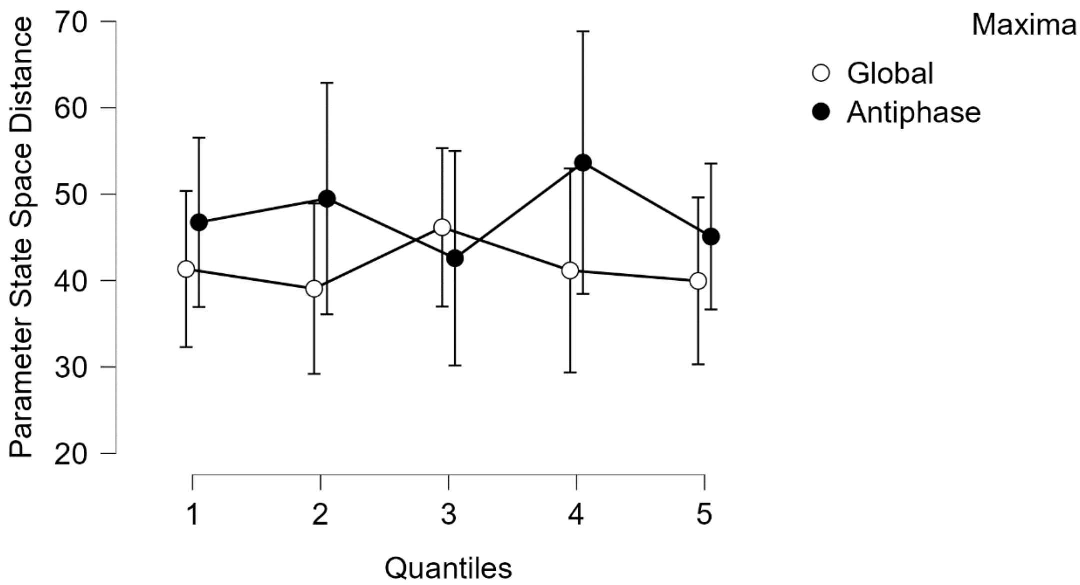

Figure 19. Line graph showing average distance to the global maximum and the antiphase maximum for selected strategies per quintiles.

Next, we compared the results from Experiment 1 with that of Experiment 2 to examine the effect of the intention manipulation. First, we looked at the differences in selected strategies' absolute mutual information over quantiles between Experiment 1 and 2. The 2 (Experiment) x 5 (Quintile) mixed ANOVA showed a significant main effect of Quintiles, F (4,108) = 5.83, p < .001. The mean absolute mutual information at the first quintile (M = 2.11, SD = .33) was significantly lower than that of the third (M = 2.22, SD = .33), fourth (M = 2.24, SD = .33), and fifth (M = 2.25, SD = .33) quintiles. There was a significant main effect of Experiment, F (1,27) = 6.51, p = .017. Absolute mutual information in Experiment 1 (M = 2.10, SD = .27) was significantly lower than that in Experiment 2 (M = 2.33, SD = .32). We also found a significant interaction effect between Experiment and Quintiles, F (4,108) = 6.55, p < .001. Differences in absolute mutual information between Experiment 1 and Experiment 2 were greater in early trials compared to later trials (see Figure 20).

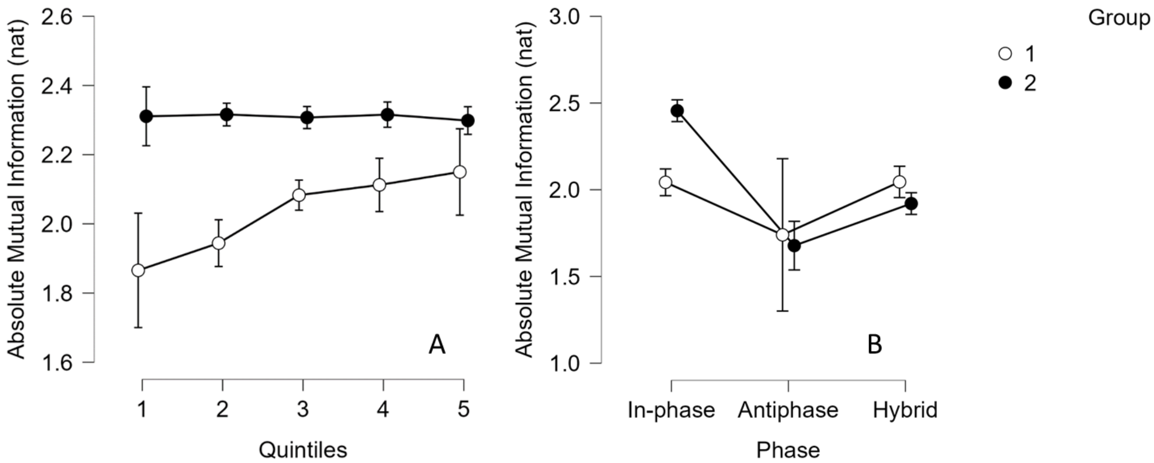

Figure 20. Comparisons of absolute mutual information between Experiment 1 and Experiment 2. (A) Line graph showing absolute mutual information as a function of Quintiles and Experiment (1 and 2). (B) Line graph showing absolute mutual information as a function of Phase (In-phase, antiphase, and hybrid) and Experiment (1 and 2).

We predicted that the mutual information of selected strategies in Experiment 2 would be lower than those in Experiment 1. However, the results showed that the absolute mutual information of selected strategies in Experiment 2 were consistently higher across trials. To further elucidate the source of this difference, we performed an additional 2 (Experiment) x 3 (Phase) mixed ANOVA comparing the mutual information of strategies between the first and second Experiment, according to the types of movement. We found that the mutual information of antiphase and hybrid trials were equal across Experiments. In contrast, the mutual information of in-phase trials was significantly higher in Experiment 2, t (2) = 6.55, $p < .001$. Overall, the results were in the opposite direction from what we had predicted.

For relative mutual information, we used a 2 (Experiment) x 5 (Quintiles) mixed ANOVA. The test found no significant main effect of Quintiles, F (4,80) = .36, p = .840, nor a main effect of Experiment, F (1,20) = .34, p = .567. There was no significant interaction effect either, F (4,80) = .75, p = .561. Relative mutual information for participants' chosen strategies was not influenced by intention manipulation or trial.

We next looked at the distance of selected strategies to the global maximum. The 2 (Experiment) x 5 (Quintiles) mixed ANOVA indicated no significant main effect of Quintiles, F (4,80) = .18, p = .947, or a main effect of Experiment, F (1,20) = 2.39, p = .138. The interaction effect was also not significant, F (4,80) = .92, p = .457. The distance between participants' chosen strategies and the global maxima was not influenced by intention manipulation or trial order.

We looked at the distance of selected strategies to the antiphase maximum. Results from the 2 (Experiment) x 5 (Quintiles) mixed ANOVA once again showed no significant main effect of Quintiles F (4,80) = .40, p = .810, or a main effect of Experiment, F (1,20) = .05, p = .835. There was also no significant interaction effect between Experiment and Quintiles, F (4,80) = .63, p = .641. Similar to distance to the global maximum, there was no indication that distance to the antiphase maximum was influenced by intention manipulation or trial order.

We predicted that participants' selected strategies in Experiment 2 would be closer to the antiphase maximum and further away from the global maximum than strategies selected in Experiment 1. The results did not indicate a significant shift in the distribution of selected control strategies towards the antiphase region of parameter state space.

Discussion

Experiment 2 was designed to assess the extent to which a shift in intention can bias the selection of control strategies in interactions with complex systems. Findings from the literature demonstrated that the selection of stable control strategies relies on optimizing for predictability (Maurice et al., 2018; Bazzi & Sternad, 2020). However, we argued that additional goals, constraints, or action intentions, (e.g., “move the object so that it remains within this boundary”, or “move the object as quickly as you can”) can also influence the selection of control strategies. To examine whether intentional shift can influence interactions with a complex system, and whether such manipulation can cause participants to violate the predictability principle, we introduced a speed incentive to the task of controlling the cart-pendulum system. We hypothesized that a shift in intention can encourage exploration of different control strategies, thus leading to more frequent discovery and execution of the high-frequency anti-phase control pattern. However, intention cannot push the system into control strategies that lack predictability, considering the traditional goals of such systems in regulating balance and locomotion of the body in daily scenarios.

The results showed some evidence suggesting that the shift in intention influenced interactions with the cart-pendulum system. The manipulation was successful in encouraging participants to perform at higher movement frequencies than they did in Experiment 1. Consistent with our prediction, the intention manipulation also caused a substantial increase in the proportion of trials that used the antiphase or hybrid strategies, compared to the distribution in Experiment 1. However, we did not find significant shifts of selected strategies towards the antiphase region on the parameter state space. A possible explanation for this inconsistency is that a large proportion of trials with antiphase (46.36%) and hybrid (84.5%) were not included in the distance analyses due to poor model fits. The inclusion of these trials may lead to results that are consistent with our finding on the shift to antiphase and hybrid patterns.

We also predicted that the intention manipulation would only cause participants to shift selected strategies among stable patterns of control (as identified by Wallace et al., 2021). That is, we predicted that participants would seek a compromise between high frequency and high predictability, rather than completely abandon predictability when frequency was prioritized. We also expected to see overall lower mutual information in Experiment 2 due to greater usage of the antiphase and hybrid movement patterns. We found that all trials fit into one of the three previously identified movement patterns. However, we did not find lower mutual information when comparing the selected strategies of Experiment 2 against those selected in Experiment 1. Rather, the mutual information of selected strategies in Experiment 2 were significantly higher across trials when compared to Experiment 1. Further analysis revealed that although mutual information in antiphase and hybrid trials were similar across Experiments, mutual information measured on in-phase trials in Experiment 2 was significantly higher than in Experiment 1. This result can be interpreted as a compensatory mechanism, where participants attempted to make up for losses in predictability due to higher movement frequencies by seeking higher mutual information strategies within each movement pattern. This interpretation is in line with discussion by van Orden et al. (2003) and

Likens et al. (2015), where pressure on a complex system from intention, environmental constraints, and control may give rise to more nested and highly coordinated behavioral patterns.

CHAPTER 4

CONCLUSION

Recent efforts in modeling human interactions with complex objects showed that people prioritize predictability over other optimization goals typically associated with centralized control models (Maurice et al., 2018; Bazzi & Sternad, 2020; Wallace et al., 2021). Furthermore, people rely on the inherent constraints and dynamics of the system's behaviors to find control strategies that are highly stable and predictable. This view is consistent with the dynamical systems approach (Bernstein, 1967; Mitra et al., 1998; Newell & Vaillancourt, 2001; van Orden et al., 2003). In this paper, we looked at the role of predictability in two instances: when information about the system is limited, and when additional constraint from intention is imposed on the system.

In Experiment 1, we considered the method that participants used to formulate and optimize for control strategies with high predictability during initial interactions with a novel, complex object. In this scenario, where information about the system's properties and dynamics are missing, participants may make use of their pre-existing knowledge and gathered information to construct a rudimentary model of the system (Osiurak & Badets, 2016; Goldenberg, 2013; Buxbaum, 2001; Thill et al., 2013; Kawato & Wolpert, 1998, Dingwell et al., 2002, 2004; Danion et al., 2012), which can be used to generate a control vector. Alternately, participants could restrict a part of their movements to simplify the system's reaction, then gradually adjust control strategy until predictability improves (Bernstein, 1967; Newell & Vaillancourt, 2001).

We generated two series of simplified models based on these principles, then compared the model-recommended solutions with strategies selected by participants. The results indicated that participants were not sensitive to the dynamics of our internally constructed, simplified models. That is, participants' selected strategies did not gravitate towards regions of high mutual information within these simplified models. However, when we mapped participants' strategies onto models with restricted movement, we found that the selected strategies adhered closely to regions of high mutual information. Taken as a whole, these findings suggested that the complexity of the system is mitigated at the biomechanical periphery to allow for the inherent interaction dynamics to unfold. This finding is consistent with a wealth of evidence from studies in the dynamical systems perspective which showed similar peripheral restrictions during early learning of novel movement patterns (Vereijken et al., 1992; Mcdonald et al., 1989; Steenbergen et al., 1995), as well as from studies of embodied tool use (Martel et al., 2006).

In Experiment 2, we considered the role of predictability alongside that of intention in controlling complex objects. Thill et al.'s (2013) defined intention as an internal state, distinct from environmental context, that can be altered by instructions. However, intention can also be considered to be a system constraint that restricts the range of possible control strategies to only those that satisfy the task requirements (Newell, 2003). Although the effect of intention on interactions with simple objects was well-documented (see Tipper et al., 2006; Costantini et al., 2010), its influence on interactions with complex objects is less clear. Furthermore, what will happen if verbal instructions compete with the predictability principle? Will the principle of predictability be eschewed in favor of the new intentional state, or will people seek compromises that accommodate the new constraint? Our findings suggested that a shift in intention (in the form of an incentive to speed up movement frequency) can cause people to find and adopt more unstable but higher performing control strategies. In addition to this tradeoff between performance and control, we also found that people were compensating for the potential loss of predictability by seeking control strategies with higher predictability in easier movement patterns.

Across two Experiments, we examined two specific instances where the role of predictability in control of complex objects was unclear. Looking at the big picture, it is evident that the selection and execution of control strategies rely on optimization for predictability, and that such optimization can be achieved by adjustments at the biomechanical periphery. Furthermore, predictability remains an important goal in control of complex objects, even when additional constraints or goals may prioritize other qualities in a control strategy.

These findings may also have broader implications for our understanding of interactions with similarly complex systems, most notably of our own body. One of the central impetuses for studying complex objects is the fact that their nested, interaction-dominant dynamics resemble that of the body, itself a complex dynamical system (Bazzi & Sternad, 2020). Solving problems of control for such complex objects then requires us to consider many of the same difficulties that researchers face when studying motor control (Schaal et al., 2007). The natural extension of this line of research is then to make explicit this potential link.

Limitations and Future Directions

One of the main issues with our data is that a large proportion of the data followed the hybrid movement pattern, a pattern that was previously not reported in studies using the same model. This movement pattern contains aspects of both in-phase and antiphase patterns. Its relative phase oscillates between these two states, and its observed frequency falls between the observed frequency for in-phase and antiphase. During data collection, we observed several participants independently adopted this strategy and successfully maintained it over multiple trials. Because our model frequently failed to generate an adequate fit for this pattern, a large number of trials in this pattern were excluded from the data. Because this movement pattern both exhibits higher movement frequency (which aligns with our intention manipulation) and lies between in-phase and antiphase patterns, exclusion of these trials can potentially influence the results of Experiment 2.

The prevalence and performance of this movement pattern suggest that this is a stable and high performing strategy. However, we have only found one mention of this pattern in simulation data (Wallace et al., 2021), not in data collected in experimental settings. One possible explanation is the fact that the apparatus used in the current series of experiments involved physical objects, whereas previous studies using this model employed robotic manipulandum, which removed both friction and movement along the longitudinal axis (Maurice et al., 2018; Bazzi & Sternad, 2021). The conditions under which the hybrid movement pattern becomes the favored pattern of movement could be an interesting topic for future research. For now, one of our main goals moving forward is to look at model modifications that account for this pattern of data. Refer to Appendix I for our current attempt at improving the model.

Another limitation of the current study involves the calculation of relative distances. Current calculations of relative distances used K and B values that were specific to each trial. However, due to constraints on time and computational power, all other parameters were fixed to a common, averaged value. This results in relative distances that were potentially incorrect. Since the methods used in this paper can be readily extended to multi-dimensional matrices, one of our next steps is to allocate resources to calculating the mutual information values for each combination of K, B, f, and A, (instead of just K and B currently) in order to obtain accurate measures of relative distance between different strategies selected by participants.

Conclusion

The findings presented in this paper reinforced predictability as an important principle in control of complex objects. Generalizing these techniques and findings across domains may prompt beneficial development in our understanding of interactions with other complex systems. Considering the potential impact that a better understanding of some complex systems (such as self-driving vehicles, climate, or social media) may have on our society, further research utilizing this paradigm may prove to be crucial to our ability to find solutions for modern issues.

REFERENCES

Abraham, R. H. & Shaw, C. S. (1992). Dynamics - The Geometry of Behavior. Adison-Wesley Publishing Company.

Adam, J. A. (1971). A closed-loop theory of motor learning. Journal of Motor Behavior, 3(2), 111-150.

Amazeen, P. G., Amazeen, E. L., & Turvey, M. T. (1998). Dynamics of human intersegmental coordination: Theory and research. In D. A. Rosenbaum & C. E. Collyer (Eds.), Timing of behavior: Neural, psychological, and computational perspectives (pp. 237–259). The MIT Press.

Arutyunyan, G. A., Gurfinkel, V. S., & Mirskii, M. L. (1968). Study of taking aim at a target. Biophysics, 13(3), 642-645.

Baccarini, M., Martel, M., Cardinali, L., Sillan, O., Farnè, A., & Roy, A. C. (2014). Tool use imagery triggers tool incorporation in the body schema. Frontiers in psychology, 5, 492.

Bazzi, S., & Sternad, D. (2020). Human control of complex objects: towards more dexterous robots. Advanced Robotics, 34(17), 1137-1155.

Bernstein, N.A. (1967). The co-ordination and regulation of movement. Pergamon Press,

Borghi, A. M. (2004). Object concepts and action: Extracting affordances from objects parts. Acta Psychologica, 115(1), 69-96.

Buxbaum, L. J. (2001). Ideomotor apraxia: a call to action. Neurocase, 7(6), 445-458.

Cabrera, J. L., & Milton, J. G. (2004). Human stick balancing: tuning Lévy flights to improve balance control. Chaos: An Interdisciplinary Journal of Nonlinear Science, 14(3), 691-698.

Cardinali, L., Frassinetti, F., Brozzoli, C., Urquizar, C., Roy, A. C., & Farnè, A. (2009). Tool-use induces morphological updating of the body schema. Current biology, 19(12), R478-R479.

Costantini, M., Ambrosini, E., Tieri, G., Sinigaglia, C., & Committeri, G. (2010). Where does an object trigger an action? An investigation about affordances in space. Experimental Brain Research, 207(1), 95-103.

Cover, T. M., & Gopinath, B. (Eds.). (2012). Open problems in communication and computation. Springer Science & Business Media.

Danion, F., Diamond, J. S., & Flanagan, J. R. (2012). The role of haptic feedback when manipulating nonrigid objects. Journal of neurophysiology, 107(1), 433-441.

d'Avella, A., Saltiel, P., & Bizzi, E. (2003). Combinations of muscle synergies in the construction of a natural motor behavior. Nature neuroscience, 6(3), 300-308.

Del Sole, T. (2004). Predictability and information theory. Part I: Measures of predictability. Journal of the atmospheric sciences, 61(20), 2425-2440.

Desmurget, M., & Grafton, S. (2000). Forward modeling allows feedback control for fast reaching movements. Trends in cognitive sciences, 4(11), 423-431.

Dingwell, J. B., Mah, C. D., & Mussa-Ivaldi, F. A. (2002). Manipulating objects with internal degrees of freedom: evidence for model-based control. Journal of Neurophysiology, 88(1), 222-235.

Dingwell, J. B., Mah, C. D., & Mussa-Ivaldi, F. A. (2004). Experimentally confirmed mathematical model for human control of a non-rigid object. Journal of Neurophysiology, 91(3), 1158-1170.

Dotov, D., Nie, L., Wojcik, K., Jinks, A., Yu, X., & Chemero, A. (2017). Cognitive and movement measures reflect the transition to presence-at-hand. New Ideas in Psychology, 45, 1-10.

Flanagan, J. R., & Wing, A. M. (1997). The role of internal models in motion planning and control: evidence from grip force adjustments during movements of hand-held loads. Journal of Neuroscience, 17(4), 1519-1528.

Gibbons, C. T., Amazeen, P. G., & Jondac, J. J. (2019). Thinking on your feet: An analysis of movement and cognition in a sit to stand task. Acta psychologica, 192, 52-58.

Gibson, J. J. (1979). The ecological approach to visual perception. Boston, Houghton Mifflin.

Goldenberg, G. (2013). Apraxia: The cognitive side of motor control. Oxford University Press.

Gorman, J. C., Amazeen, P. G., & Cooke, N. J. (2010). Team coordination dynamics. Nonlinear Dynamics, Psychology, and Life Sciences, 14(3), 265.

Gorman, J. C., Cooke, N. J., Amazeen, P. G., & Fouse, S. (2012). Measuring patterns in team interaction sequences using a discrete recurrence approach. Human Factors, 54(4), 503-517.

Haken, H., Kelso, J. S., & Bunz, H. (1985). A theoretical model of phase transitions in human hand movements. Biological cybernetics, 51(5), 347-356.

Heuer, H. (1994). On How to Get What One Wants. Applied Psychology, 43(3), 382-386.

Holst E von (1937/1973) On the nature and order of the central nervous system. In: Martin R (ed) The collected papers of Erich von Holst, vol. 1. The behavioral physiology of animal and man. University of Miami Press.

Huang, F. C., Gillespie, R. B., & Kuo, A. D. (2007). Visual and haptic feedback contribute to tuning and online control during object manipulation. Journal of motor behavior, 39(3), 179-193.

Kawato, M., & Wolpert, D. (1998). Internal models for motor control. Sensory guidance of movement, 218, 291-307.

Kelso, J. A. (1984). Phase transitions and critical behavior in human bimanual coordination. American Journal of Physiology-Regulatory, Integrative and Comparative Physiology, 246(6), R1000-R1004.

Kelso, J. S. (1995). Dynamic patterns: The self-organization of brain and behavior. MIT press.

Kugler, P. N., & Turvey, M. T. (1987). Information, natural law and the self-assembly of rhythmic movement. Hillsdale, NJ: Erlbaum. Oxford.

Lacquaniti, F. (1989). Central representations of human limb movement as revealed by studies of drawing and handwriting. Trends in Neurosciences, 12(8), 287-291.

Lee, D. N. (1976). A theory of visual control of braking based on information about time-to-collision. Perception, 5(4), 437-459.

Lee, D. N., & Reddish, P. E. (1981). Plummeting gannets: A paradigm of ecological optics. Nature, 293(5830), 293-294.

Lee, T. D., Swinnen, S. P., & Verschueren, S. (1995). Relative phase alterations during bimanual skill acquisition. Journal of motor behavior, 27(3), 263-274.

Leib, R., & Karniel, A. (2012). Minimum acceleration with constraints of center of mass: a unified model for arm movements and object manipulation. Journal of Neurophysiology, 108(6), 1646-1655.

Likens, A. D., Fine, J. M., Amazeen, E. L., & Amazeen, P. G. (2015). Experimental control of scaling behavior: what is not fractal? Experimental Brain Research, 233(10), 2813-2821.

Maravita, A., & Iriki, A. (2004). Tools for the body (schema). Trends in cognitive sciences, 8(2), 79-86.

Martel, M., Cardinali, L., Roy, A. C., & Farnè, A. (2016). Tool-use: An open window into body representation and its plasticity. Cognitive neuropsychology, 33(1-2), 82-101.

Maurice, P., Hogan, N., & Sternad, D. (2018). Predictability, force, and (anti) resonance in complex object control. Journal of Neurophysiology, 120(2), 765-780.

McDonald, P. V., Van Emmerik, R. E. A., & Newell, K. M. (1989). The effects of practice on limb kinematics in a throwing task. Journal of motor behavior, 21(3), 245-264.

Mitra, S., Amazeen, P. G., & Turvey, M. T. (1998). Intermediate motor learning as decreasing active (dynamical) degrees of freedom. Human movement science, 17(1), 17-65.

Mosier, K., Lau, C., Wang, Y., Venkadesan, M., & Valero-Cuevas, F. J. (2011). Controlling instabilities in manipulation requires specific cortical-striatal-cerebellar networks. Journal of neurophysiology, 105(3), 1295-1305.

Nasseroleslami, B., Hasson, C. J., & Sternad, D. (2014). Rhythmic manipulation of objects with complex dynamics: predictability over chaos. PLoS Computational Biology, 10(10), e1003900.

Newell, K. M. (2003). Schema theory (1975): Retrospectives and prospectives. Research quarterly for exercise and sport, 74(4), 383-388.

Newell, K. M., & Vaillancourt, D. E. (2001). Dimensional change in motor learning. Human movement science, 20(4-5), 695-715.

Newell, K. M., & Valvano, J. (1998). Movement science: therapeutic intervention as a constraint in learning and relearning movement skills. Scandinavian Journal of Occupational Therapy, 5(2), 51-57.

Osiurak, F., & Badets, A. (2016). Tool use and affordance: Manipulation-based versus reasoning-based approaches. Psychological review, 123(5), 534.

Osiurak, F., Aubin, G., Allain, P., Jarry, C., Richard, I., & Le Gall, D. (2008). Object utilization and object usage: A single-case study. Neurocase, 14(2), 169-183.

Osiurak, F., Jarry, C., & Le Gall, D. (2010). Grasping the affordances, understanding the reasoning: toward a dialectical theory of human tool use. Psychological review, 117(2), 517.

Pagano, C. C. (1993). Inertial eigenvectors as the basis for the perception of limb direction (Doctoral dissertation, University of Connecticut).

Rand, R. H., Cohen, A. H., & Holmes, P. J. (1988). Systems of coupled oscillators as models for central pattern generators. In: Cohen AH, Rossignol S, Grillner S, editors. Neural control of rhythmic movements in vertebrates. New York: Wiley; 1988. pp. 333–367.

Roerdink, M., De Haart, M., Daffertshofer, A., Donker, S. F., Geurts, A. C. H., & Beek, P. J. (2006). Dynamical structure of center-of-pressure trajectories in patients recovering from stroke. Experimental brain research, 174(2), 256-269.

Schaal, S., Mohajerian, P., & Ijspeert, A. (2007). Dynamics systems vs. optimal control—a unifying view. Progress in brain research, 165, 425-445.

Schmidt, R. A. (1975). A schema theory of discrete motor skill learning. Psychological Review, 82, 225-260.

Schmidt, R. A. (1985). The search for invariance in skilled movement behavior. Research Quarterly for Exercise and Sport, 56, 188-200.

Schneider, K., & Zernicke, R. F. (1989). Jerk-cost modulations during the practice of rapid arm movements. Biological Cybernetics, 60(3), 221-230.

Scholz, J. P., & Schöner, G. (1999). The uncontrolled manifold concept: identifying control variables for a functional task. Experimental brain research, 126(3), 289-306.

Scott, S. Optimal feedback control and the neural basis of volitional motor control. Nat Rev Neurosci 5, 532–545 (2004). https://doi.org/10.1038/nrn1427

Shannon, C. E. (1948). A mathematical theory of communication. The Bell system technical journal, 27(3), 379-423.

Shaw, R. E., Turvey, M. T. & Mace, W. M. (1982). Ecological psychology. The consequence of a commitment to realism. In W. Weimer & D. Palermo (Eds.) Cognition and the symbolic processes, vol. 2, 159 – 226.

Shea, C. H., & Wulf, G. (2005). Schema theory: A critical appraisal and reevaluation. Journal of motor behavior, 37(2), 85-102.

Slota, G. P., Latash, M. L., & Zatsiorsky, V. M. (2011). Grip forces during object manipulation: experiment, mathematical model, and validation. Experimental Brain Research, 213(1), 125-139.

Smith, L. B., & Thelen, E. E. (1993). A dynamic systems approach to development: Applications. In This book grew out of a workshop," Dynamic Systems in Development," held for the Society for Research in Child Development in Kansas City, KS, Apr 1989. The MIT Press.

Southard, D., & Higgins, T. (1987). Changing movement patterns: Effects of demonstration and practice. Research quarterly for exercise and sport, 58(1), 77-80.

Steenbergen, B., Marteniuk, R. G., & Kalbfleisch, L. E. (1995). Achieving coordination in prehension: Joint freezing and postural contributions. Journal of motor behavior, 27(4), 333-348.

Stergiou, N., & Decker, L. M. (2011). Human movement variability, nonlinear dynamics, and pathology: is there a connection? Human movement science, 30(5), 869-888.

Svinin, M., Goncharenko, I., Kryssanov, V., & Magid, E. (2019). Motion planning strategies in human control of non-rigid objects with internal degrees of freedom. Human Movement Science, 63, 209-230.

Symes, E., Ellis, R., & Tucker, M. (2007). Visual object affordances: Object orientation. Acta psychologica, 124(2), 238-255.

Thelen, E., & Smith, L. B. (1994). A dynamic systems approach to the development of cognition and action. MIT press.

Thelen, E., Schöner, G., Scheier, C., & Smith, L. B. (2001). The dynamics of embodiment: A field theory of infant perseverative reaching. Behavioral and Brain Sciences, 24(1), 1-34.

Thill, S., Caligiore, D., Borghi, A. M., Ziemke, T., & Baldassarre, G. (2013). Theories and computational models of affordance and mirror systems: an integrative review. Neuroscience & Biobehavioral Reviews, 37(3), 491-521.

Ting, L. H., & McKay, J. L. (2007). Neuromechanics of muscle synergies for posture and movement. Current opinion in neurobiology, 17(6), 622-628.

Tucker, M., & Ellis, R. (1998). On the relations between seen objects and components of potential actions. Journal of Experimental Psychology: Human perception and performance, 24(3), 830.

Turvey, M. T. (1990). Coordination. American Psychologist, 45(8), 938–953. https://doi.org/10.1037/0003-066X.45.8.938

Turvey, M. T. (1994). From Borelli (1680) and Bell (1826) to the Dynamics of Action and Perception. Journal of Sport & Exercise Psychology, 16.

van Orden, G. C., Holden, J. G., & Turvey, M. T. (2003). Self-organization of cognitive performance. Journal of Experimental Psychology: General, 132(3), 331.

Von Holst, E. (1973). The reafference principle. The Behavioral Physiology of Animals and Man.

Vereijken, B., Emmerik, R. E. V., Whiting, H. T. A., & Newell, K. M. (1992). Free (z) ing degrees of freedom in skill acquisition. Journal of motor behavior, 24(1), 133-142.

Wallace, B., Kong, L. W., Rodriguez, A., & Lai, Y. C. (2021). Synchronous transition in complex object control. Physical Review Applied, 16(3), 034012.

Warren, W. H. (1984). Perceiving affordances: visual guidance of stair climbing. Journal of experimental psychology: Human perception and performance, 10(5), 683.

APPENDIX A

IMPROVEMENTS TO CART-PENDULUM MODEL TO ACCOMMODATE HYBRID MOVEMENT PATTERN

A large proportion of trials across both Experiment 1 (47.7%) and 2 (61.4%) exhibited the hybrid movement pattern. However, the cart-pendulum model was only able to generate good fits for a small percentage (14.94% for Experiment 1, 15.5% for Experiment 2) of trials with this movement pattern. Here, we outlined the different methods attempted to improve model fit for the hybrid movement pattern.

General model fitting procedure

Following the procedure outlined in Maurice et al. (2018), we used the following settings to search for parameters that would generate the best fit with the observed data. From the 45-second movement signals, a 20-second segment was selected, starting from 15 seconds from the beginning of the trial to 10 seconds before the end of the trial. This was performed on all four vectors that specified the cart-pendulum system's state: cart position, cart velocity, pendulum phase angle, and pendulum phase angle velocity (see Figure 7 for an example, and Figure A1 for a zoomed in cut of a similar trial). These data segments were subjected to a 5-point moving average smoothing function to remove potential instrument noise. Then, we tasked the model to search for the pair of K and B parameters that would produce the best fitting vectors to the observed data. Fit was calculated as the average of the root mean square residuals between the four model generated vectors and observed data. The K and B parameter values were randomly picked between 0 and 30 for K, and between 0 and 3 for B. We used MATLAB's MultiStart function to generate 50 random starting values of K and B, and allowed the model to search for 1000 iterations per starting point.

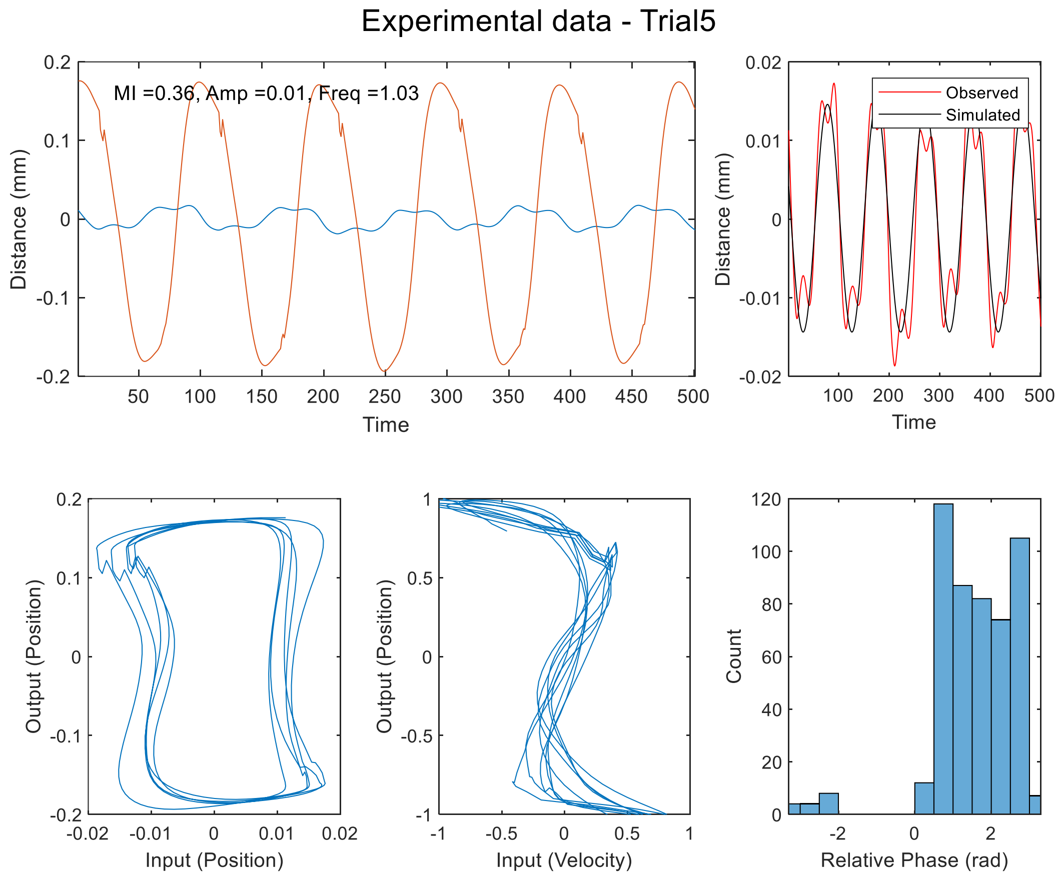

Figure A1. Raw data signals for and preliminary analyses for Participant 3, trial 5. The top left panel shows the input cart position vector (blue) and output pendulum phase angle (red).

Smoothing

By default, a 5-point moving average smoothing function was applied to the raw movement signals. We noticed smaller troughs at the peaks of each movement cycle, which can often also be found at the endpoints of simple movements. Such instances of "double-peaking" can be corrected using higher number of points for the smoothing function. Smoothing functions with moving average of up to 20 points were attempted, which noticeably washed out the smaller troughs at peak movements (see Figure A2). We found no improvement to the model fit.

Window of observation

We attempted to shift the window of observation (from between 15 seconds and 35 seconds) to several other starting and ending points. However, because participants who performed the hybrid pattern did so consistently throughout their trials, this method did not yield noticeable changes to the model fit.

Parameter range

We attempted to expand the search range for the K and B parameters to values beyond 30 N/m (for K) and 3 N.s/m (for B). Search range for up to 300 N/m (the equivalent to 30 kilograms-force) and 30 N.s/m was used. Not only were these amounts of force far beyond what should be expected in the experiment, given the nature of the task, but the increase in value also did not fundamentally change the relative dynamics between the cart-pendulum parts. As such, increases of parameter range was not a viable strategy to improve model fit.

Increasing frequency

Wallace et al. (2021) mentioned a pattern similar to the hybrid pattern we observed in our experiment. This pattern was found in parameter regions between the common in-phase and antiphase patterns. The authors created this pattern in their simulation of the model by altering the oscillatory frequency of the input cart vector. Although frequency was fixed in our experiment with the help of a metronome, if we consider the small troughs at each movement peak as an additional cycle, an increase in frequency could be justified. We gradually increased the frequency of the input vector and monitored the model-generated output. At between 3.4 to 3.8Hz (about 3 to 4 times the original estimated frequency), we obtained model solutions that were closer to the observed data (see Figure A3). However, closer inspection of the input position vector revealed that an increase in frequency was not sufficient due to the additional asymmetry of the observed data (for example, Figure A3, observed position vector at time 350 and 450). Despite a better fit, there were still significant deviations from the observed data.

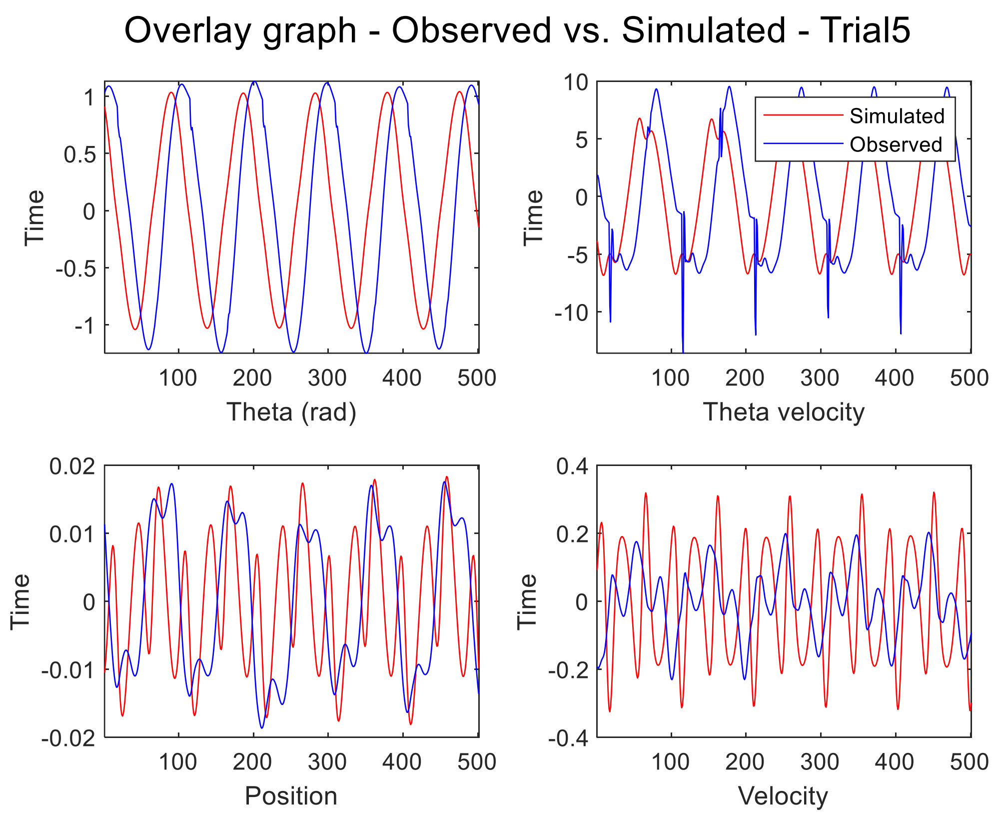

Figure A3. Model fit for the hybrid movement pattern, obtained by increasing frequency f.

Non-linear escapement terms

Asymmetry in the position vector can be implemented in the model by changing equation 5 to include nonlinear escapement terms. We attempted to adapt two nonlinear modifications to the standard mass spring model: Rayleigh and Van der Pol (Abraham & Shaw, 1992). However, both modifications did not alter the dynamics of the model-generated vectors in the direction of the observed data. See example of the Rayleigh modification (Figure A4) and the Van der Pol modification (Figure A5).

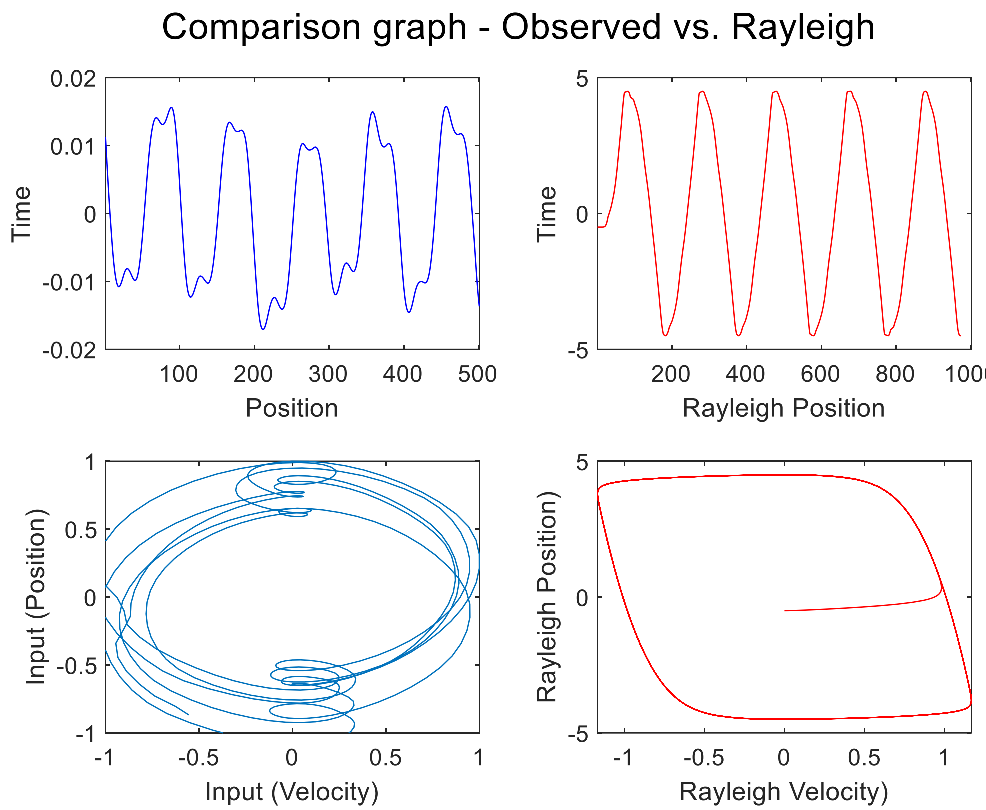

Figure A4. Comparison of observed input vector (top left) and input phase portrait (bottom left) against the Rayleigh input vector (top right) and Rayleigh input phase portrait (bottom right).

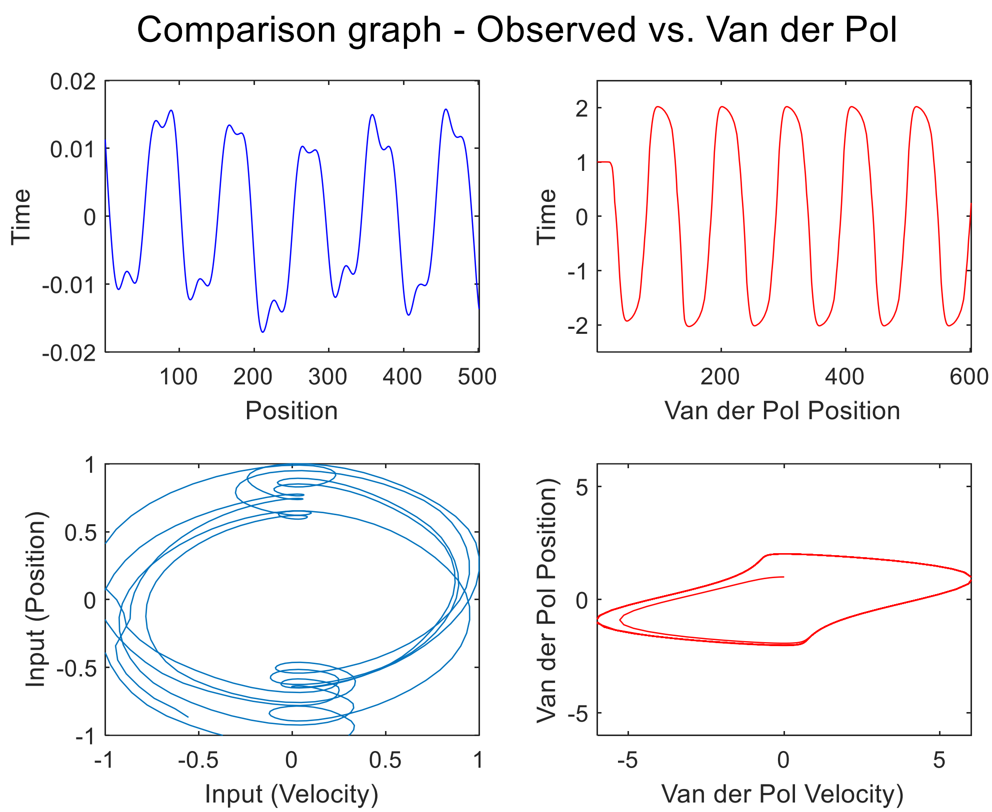

Figure A5. Comparison of observed input vector (top left) and input phase portrait (bottom left) against the Van der Pol input vector (top right) and Van der Pol input phase portrait (bottom right).